Developmental Biology 406 (2015) 14–39

Contents lists available at ScienceDirect

Developmental Biology

journal homepage: www.elsevier.com/locate/developmentalbiology

# Lineage-associated tracts defining the anatomy of the *Drosophila* first instar larval brain

Volker Hartenstein [a,*], Amelia Younossi-Hartenstein [a], Jennifer K. Lovick [a], Angel Kong [a], Jaison J. Omoto [a], Kathy T. Ngo [a], Gudrun Viktorin [b]

[a] *Department of Molecular Cell and Developmental Biology, University of California, Los Angeles, 610 Charles E. Young Drive, 5009 Terasaki Life Sciences Building, Los Angeles, CA 90095, USA*
[b] *Biozentrum, University of Basel, Basel, Switzerland*

ARTICLE INFO

*Article history:*
Received 21 April 2015
Received in revised form
25 June 2015
Accepted 27 June 2015
Available online 30 June 2015

*Keywords:*
Brain
Development
*Drosophila*
Larval
Lineage

ABSTRACT

Fixed lineages derived from unique, genetically specified neuroblasts form the anatomical building blocks of the *Drosophila* brain. Neurons belonging to the same lineage project their axons in a common tract, which is labeled by neuronal markers. In this paper, we present a detailed atlas of the lineage-associated tracts forming the brain of the early *Drosophila* larva, based on the use of global markers (anti-Neuroglian, anti-Neurotactin, *inscuteable*-Gal4 > UAS-chRFP-Tub) and lineage-specific reporters. We describe 68 discrete fiber bundles that contain axons of one lineage or pairs/small sets of adjacent lineages. Bundles enter the neuropil at invariant locations, the lineage tract entry portals. Within the neuropil, these fiber bundles form larger fascicles that can be classified, by their main orientation, into longitudinal, transverse, and vertical (ascending/descending) fascicles. We present 3D digital models of lineage tract entry portals and neuropil fascicles, set into relationship to commonly used, easily recognizable reference structures such as the mushroom body, the antennal lobe, the optic lobe, and the Fasciclin II-positive fiber bundles that connect the brain and ventral nerve cord. Correspondences and differences between early larval tract anatomy and the previously described late larval and adult lineage patterns are highlighted. Our L1 neuro-anatomical atlas of lineages constitutes an essential step towards following morphologically defined lineages to the neuroblasts of the early embryo, which will ultimately make it possible to link the structure and connectivity of a lineage to the expression of genes in the particular neuroblast that gives rise to that lineage. Furthermore, the L1 atlas will be important for a host of ongoing work that attempts to reconstruct neuronal connectivity at the level of resolution of single neurons and their synapses.



## 1. Introduction

As a member of the holometabolan insects, *Drosophila* fashions two different bodies during its life cycle. Living on or inside its food source, the larval body is designed for rapid ingestion of food and growth. The larva lacks segmental appendages for locomotion, and complicated sensory systems, like compound eyes or the (auditory) Johnston's organ, which, in the adult, are required for detecting food sources, mates and enemies. Corresponding to the lesser demands on controlling such complex behaviors, the early larval central nervous system is more than 1 order of magnitude smaller in size and neuronal number than its adult counterpart. However, in part because of its lower complexity, the larval brain has become a promising model system to address problems of neural structure and development, neural function, and behavior. Most of the individual larval sensory organs (sensilla), muscles, and motor neurons have been reconstructed at single cell resolution (Ghysen et al., 1993; Hartenstein, 1988; Kim et al., 2009; Landgraf et al., 2003a; Liu et al., 2003; Johansen et al., 1989; Kwon et al., 2011; Ramaekers et al., 2005; Schrader and Merritt, 2000; Sink and Whitington, 1991; Sprecher et al., 2011; Vactor et al., 1993) and their role in locomotory circuits is being established (Caldwell et al., 2003; Choi et al., 2004; Kohsaka et al., 2012). For some interneurons, including the projection neurons of the antennal lobe, the olfactory input and higher brain targets have also been mapped, and sophisticated learning paradigms are well established (Colomb et al., 2007; Gerber and Stocker, 2007; Masuda-Nakagawa et al., 2005, 2009; Python and Stocker, 2002; Schleyer et al., 2011; Selcho et al., 2009).

* Corresponding author.
*E-mail address:* volkerh@mcdb.ucla.edu (V. Hartenstein).

http://dx.doi.org/10.1016/j.ydbio.2015.06.021
0012-1606/

The *Drosophila* nervous system develops form a population of asymmetrically dividing stem cells (neuroblasts) that are born in the neurectodermal layer of the early embryo. Each of the segments of the ventral nervous system develops from 30 pairs of neuroblasts; the brain comprises approximately 100 pairs (Urbach and Technau, 2003; Younossi-Hartenstein et al., 1996). Each neuroblast is characterized by the expression of a unique combination of transcriptional regulators, and produces a structurally/functionally distinct lineage of neurons by an invariant sequence of asymmetric divisions (reviewed in Brody and Odenwald, 2005; Pearson and Doe, 2004; Urbach and Technau, 2004). A small number of 5–8 embryonic divisions generate the primary neurons that make up the larval brain (first wave of neurogenesis; Larsen et al., 2009). After a period of quiescence, these aforementioned neuroblasts reactivate in the larva and generate the much larger number of post-embryonic secondary neurons that differentiate during metamorphosis to form the adult brain (second wave of neurogenesis; Ito and Hotta, 1992; Truman and Bate, 1988; reviewed in Hartenstein et al., 2008). Neural lineages constitute developmental-genetic as well as neuro-anatomical "modules" of the developing brain. This has been studied in most detail for the secondary lineages, that were mapped at the late larval stage (Cardona et al., 2010a; Kuert et al., 2012, 2014; Pereanu and Hartenstein, 2006; Truman et al., 2004) and followed throughout metamorphosis into the adult stage (Lovick et al., 2013). The close ties between lineages and neuroanatomy can be easily appreciated at the late larval stage, where global neuronal markers, such as antibodies against the adhesion molecules Neurotactin (BP106; de la Escalera et al., 1990; Hortsch et al., 1990), Neuroglian (BP104; Bieber et al., 1989), or DE-cadherin (Dumstrei et al., 2003) show secondary lineages as cohesive clusters of immature neurons, located in the periphery of the brain (the rind or cortex; Fig. 1A–C). Neurons emit a single nerve fiber towards the brain center (the neuropil). Fibers of the same lineage form one or two tight bundles that follow an invariant trajectory by which the corresponding lineage can be recognized. These lineage-associated tracts (secondary axon tracts or SATs, for the secondary lineages) develop into the fiber bundles that connect the different neuropil compartments of the adult brain. For example, four lineages form the projection neurons connecting the antennal lobe with higher protocerebral centers, including the calyx and lateral horn (Das et al., 2013; Lai et al., 2008). In the late larva, SATs of these four lineages have extended all the way from the antennal lobe towards the target domains, bundling together into a thick tract (antennal lobe tract; ALT). During metamorphosis, dendritic and axonal branches sprout from the SATs proximally and distally, establishing the synaptic circuits within the antennal lobe and the target neuropils, respectively. Similar to the ALT, the remainder of the fiber bundles of the adult brain is formed by other lineages during the larval stage (Lovick et al., 2013; Pereanu et al., 2010).

In contrast to the now existing map of the late larval and adult brain neuropil (Pereanu and Hartenstein, 2006; Wong et al., 2013), the pattern of axon tracts formed by differentiated primary neurons in the early larva has remained relatively obscure. The structure and development of larval neuropil compartments, as well as specific "pioneer tracts" that remain visible from embryonic to larval stages, has been documented in previous works (Nassif et al., 1998, 2003; Younossi-Hartenstein et al., 2003, 2006); however, the overall projection pattern of primary lineages is not known. Primary axon tracts (PATs) of all lineages emerge during the embryonic period; like SATs, they express Neurotactin and Neuroglian, and can be visualized by antibodies against these epitopes. In the present work, we use another global neuronal marker, *insc*-Gal4, expressed neuroblasts and their neuronal progeny, visualized by membrane-localized fluorescent reporters (Betschinger et al., 2006), to follow the scaffold of secondary axon tracts backward from late to early larval stages, where it is utilized to identify the primary axon tracts. Previously, it had been shown for a few lineages (using enhancer- or promoter-Gal4 driver lines), targeted by specific molecular markers, that the SATs forming in the larva follow pre-established pathways of primary axons (Larsen et al., 2009). The findings presented here confirm this notion for lineages in general, which allowed us to generate an atlas of primary axon tracts for the L1 larval brain. A number of Gal4 driver lines expressed in subsets of lineages from early to late larval stages augmented the resolution of the atlas. We here present the pertinent features of the atlas with the help of confocal sections and digital 3D models. Our work serves the following two main purposes.

First, the L1 atlas of lineages constitutes another step towards the goal to follow lineages backward in time towards the neuroblasts of the early embryo, with the underlying objective to link each lineage (with its specific structure and connectivity) to the gene expression pattern defining the parental neuroblast. This has been recently achieved for the lineages of the ventral nerve cord (Birkholz et al., 2015), and a few select lineages of the brain, including the mushroom body (Kunz et al., 2012). In Birkholz et al. (2015), the prior use of labeled embryonic clones was instrumental to identify larval lineages with specific neuroblasts, and we anticipate the same to be true for brain lineages. Our L1 lineage atlas, translated into the late embryonic brain, will provide an anatomical scaffold with discrete landmarks to which embryonic neuroblast clones, as well as lineage-specific markers expressed from the neuroblast stage towards the late embryo, can be related.

Secondly, the atlas will significantly aid ongoing work that attempts to reconstruct neuronal connectivity at single-cell and single-synapse resolution using electron microscopy. Along this line, projects are currently under way where complete series of contiguous ultrathin sections of early larval brains are recorded by transmission electron microscopy (TEM), assembled and registered using specialized software, and digitally reconstructed (Cardona et al., 2010b, 2012). This reconstruction will be greatly aided by the anatomical landmarks provided by the lineage-associated tracts (PATs) charted in the present work. PATs represent easily identifiable elements of the TEM images (Cardona et al., 2010b), making it possible to identify the specific lineages they belong to by comparing the TEM dataset with appropriately oriented confocal stacks. Once identified in the TEM stack, the PATs define a dense grid of fixed "coordinates" to which ultrastructural details (e.g., specific types of synapses; sites of contact between particular neurons) can be related. More importantly, all primary neurons can be assigned to PATs, and thereby classified into groups with developmental significance. It will be possible to ask whether neurons that belong to a given lineage, or sublineage, share certain anatomical properties, such as axonal geometry, placement of synapses, and specific interacting neurons. These properties can then be correlated with the parental neuroblast gene expression patterns. This will serve as a foundation for understanding whether and how specific transcriptional regulators define the various anatomic properties within a lineage or sublineage.

## 2. Materials and methods

### 2.1. Fly lines

Flies were grown at 25 °C using standard fly media unless otherwise noted.

*en*-Gal4 (Tabata et al., 1995; #30564, Bloomington *Drosophila* Stock Center (BDSC), University of Indiana, IN, USA), FasII-Gal4 (Siebert et al., 2009), FasIII-Gal4 (Hayashi et al., 2002; #103948, BDSC), GH146-Gal4 (a gift from R.F. Stocker, University of Fribourg,

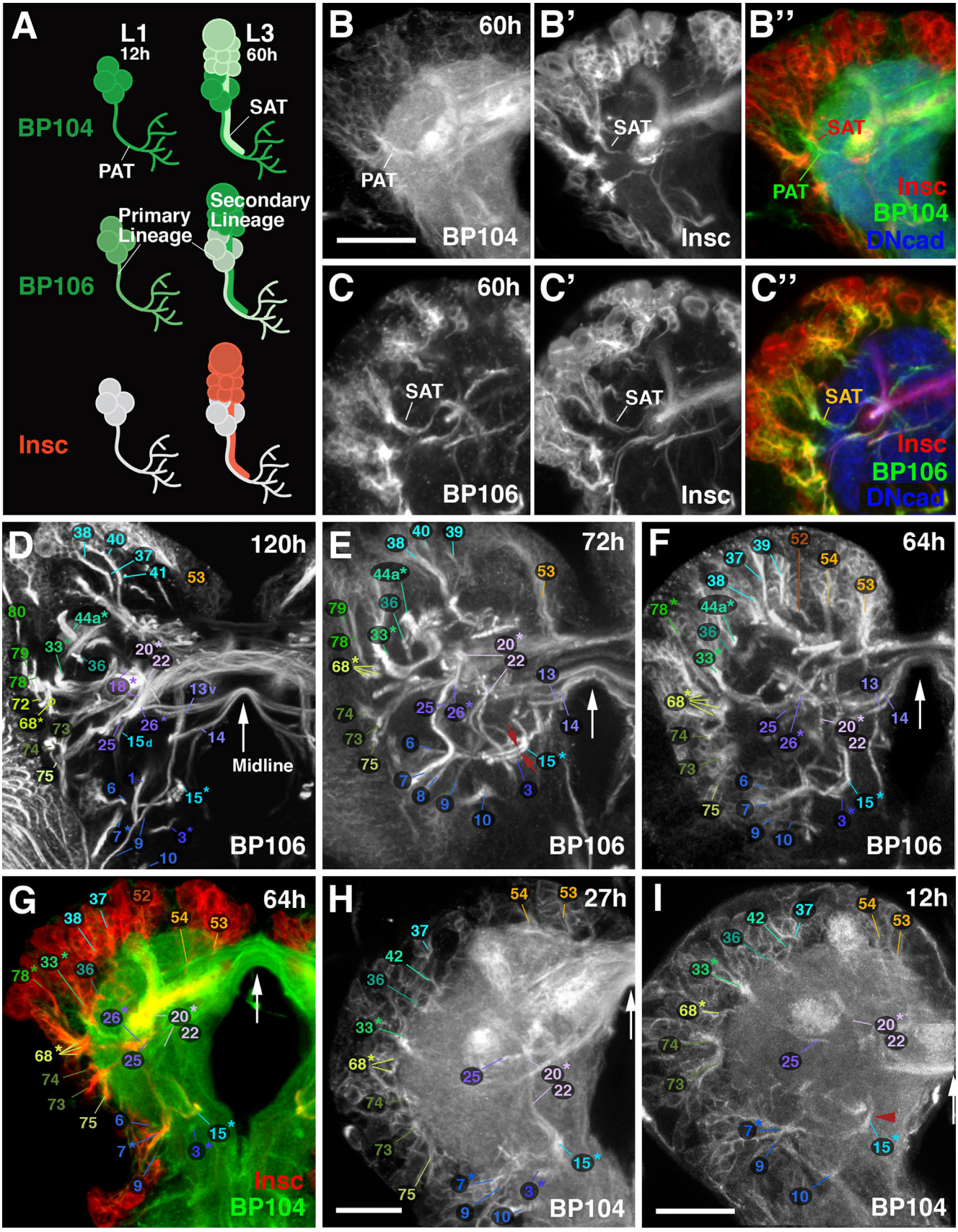
A
L1
12h
L3
60h
SAT
BP104
PAT
Primary
Lineage
Secondary
Lineage
BP106
Insc
B
60h
PAT
BP104
B'
SAT
Insc
B''
SAT
PAT
Insc
BP104
DNcad
C
60h
SAT
BP106
C'
SAT
Insc
C''
SAT
Insc
BP106
DNcad
D
120h
Midline
BP106
E
72h
BP106
F
64h
BP106
G
64h
Insc
BP104
H
27h
BP104
I
12h
BP104

Switzerland; Stocker et al., 1997), *insc*-Gal4 (Mz1407; Betschinger et al., 2006; #8751, BDSC), *per*-Gal4 (Kaneko and Hall, 2000; #7127, BDSC), *ple*-Gal4 (TH-Gal4; Friggi-Grelin et al., 2003; #8848, BDSC), *poxn*-Gal4 (Boll and Noll, 2002), R46C11-Gal4, R82E10-Gal4, R13A10-Gal4, R76A11-Gal4, R67A11-Gal4 (Janelia Farm GAL4 Stock Collection, Jenett et al. (2012); #50262 #48625 #48540 #46957 #39400, BDSC), UAS-chRFP-Tub (Rusan and Peifer, 2007; #25774, BDSC), UAS-mcd8::GFP (Lee et al., 1999; #5137, BDSC).

### 2.2. Immunohistochemistry

Samples were fixed in 4% formaldehyde or 4% methanol-free formaldehyde in phosphate buffer saline (PBS, Fisher-Scientific, pH=7.4; Cat no. #BP399-4). Tissues were permeabilized in PBT (PBS with 0.1–0.3% Triton X-100, pH=7.4) and immunohistochemistry was performed using standard procedures (Ashburner, 1989). The following antibodies were provided by the Developmental Studies Hybridoma Bank (Iowa City, IA): mouse anti-bruchpilot (nc82, 1:20), rat anti-DN-Cadherin (DN-EX #8, 1:20), mouse anti-Fasciclin II (1D4, 1:20), mouse anti-Neuroglian (BP104, 1:30), and mouse anti-Neurotactin (BP106, 1:10). Secondary antibodies, $IgG_1$ (Jackson ImmunoResearch; Molecular Probes) were used at the following dilutions: Cy5-conjugated anti-rat Ig (1:100), Cy3-conjugated anti-mouse Ig (1:200), Cy5-conjugated anti-mouse Ig (1:250); Alexa 546-conjugated anti-mouse (1:500), DynaLight 649-conjugated anti-rat (1:400), Alexa 568-conjugated anti-mouse (1:500).

### 2.3. Confocal microscopy

Staged *Drosophila* larval and adult brains labeled with suitable markers were viewed as whole-mounts by confocal microscopy [LSM 700 Imager M2 using Zen 2009 (Carl Zeiss Inc.); lenses: 40 × oil (numerical aperture 1.3)]. Complete series of optical sections were taken at 2-μm intervals. Captured images were processed by ImageJ or FIJI (National Institutes of Health, http://rsbweb.nih.gov/ij/ and http://fiji.sc/) and Adobe Photoshop.

### 2.4. Morphologically defined stages in larval brain development

Animals were staged by placing larvae hatched from the egg within a 1 h period on food plates under non crowded conditions at 25 °C. Since even when larvae are reared at low density to guarantee optimal food supply, there is a considerable variability (in the order of 10%) in brain growth of larvae of the same age. We therefore defined specific morphogenetic parameters of the rapidly expanding optic lobe as structural hallmarks of the larval brain. These parameters include the ratio of optic lobe diameter (OOA) to neuropile diameter (OOA/NP), the ratio of neuroblasts versus epithelium within the outer optic anlage (NB/NB+E), and the thickness of the layer of medulla neurons (MN; Supplementary Fig. S1A). Based on these parameters, presented in Supplementary Fig. 1B, larval brain development can be divided into 9 stages (L1A–L3E) of approximately 12 h length.

### 2.5. Generation of three-dimensional models

Digitized images of confocal sections were imported into FIJI (Schindelin et al., 2012; http://fiji.sc/). Complete series of optical sections were taken at 2-μm intervals. Since sections were taken from focal planes of one and the same preparation, there was no need for alignment of different sections. Models were generated using the 3-dimensional viewer as part of the FIJI software package. Digitized images of confocal sections were imported using TrakEM2 plugin in FIJI software (Cardona et al., 2012). Surface renderings of larval brains stained with anti-Bruchpilot were generated as volumes in the 3-dimensional viewer in FIJI. Cell body clusters were indicated on surface renderings using TrakEM2. Digital atlas models of cell body clusters and SATs were created by manually labeling each lineage and its approximate cell body cluster location in TrakEM2.

## 3. Results

### 3.1. Dynamic expression of adhesion proteins Neuroglian and Neurotactin in developing lineages

The adhesion proteins Neuroglian and Neurotactin serve as markers for the axon tracts of developing brain lineages (Lovick et al., 2013; Pereanu and Hartenstein, 2006; Truman et al., 2004). Both are expressed on neuronal somata and outgrowing neurites from mid-embryonic stages onward (Bieber et al., 1989; Hortsch et al., 1990; not shown). In the early larva, Neuroglian remains strongly expressed in primary neurons and their primary tracts (PATs; Fig. 1A, B), whereas Neurotactin is downregulated (Fig. 1A, C). Neurotactin appears again strongly in secondary neurons, which start to form at the second larval instar and produce secondary axon tracts (SATs; Fig. 1A, C). By contrast, Neuroglian expression reappears in secondary neurons at a later stage than that of Neurotactin (not shown). Similar to Neurotactin, we find that the *inscuteable*- (*insc*)-Gal4 reporter (Betschinger et al., 2006) is preferentially upregulated in secondary lineages and SATs as soon as neuroblasts enter mitosis (Fig. 1A, C′–C″). Double labelings of early larval brains, using Neuroglian (primary lineages) and *insc*-Gal4 > UAS-chRFP-Tubulin (secondary lineages), allowed us to correlate the trajectory of PATs and SATs (Fig. 1B″). For several lineages it had already been previously established that SATs follow PATs, formed by earlier born primary neurons of the same lineages, into the neuropil (Das et al., 2013; Larsen et al., 2009). Our present data demonstrate that the close association between PATs and SATs is true for almost all lineages (Fig. 1G; Supplementary Figs. S2 and S3).

**Fig. 1.** Reconstruction of lineage-associated axon tracts in the developing larval brain. (A–C″) Developing lineages labeled by three global neuronal markers: anti-Neuroglian (BP104), anti-Neurotactin (BP106), and *insc*-Gal4, UAS-chRFP-Tub. (B–B″) and (C–C″) are *z*-projections of confocal sections of a 60 h larval brain hemisphere. BP104 strongly labels primary neurons and primary axon tracts (PATs; green) in the early larva (L1 in A); it remains strongly expressed in PATs at mid larval stages (early L3; 60 h in A; B, B″). BP106 is expressed only faintly in primary neurons (A), and strongly in secondary neurons and axon tracts (SATs; green in A, right; C, C″). *insc*-Gal4 is not expressed in primary neurons of the larval brain; it only labels secondary neurons and SATs (red in A; B″; C″). Note co-labeling of PATs with BP104 and SATs with *insc*-Gal4 in panel B″. Neuropil is labeled by anti-DN-cadherin (DNcad; blue) in B″ and C″. (D–I) *z*-Projections of frontal confocal sections of larval brain hemispheres labeled with BP106 (D–F), *insc*-Gal4/BP104 (G) and BP104 (H–I). The antibodies/Gal4 drivers mark SATs (D–G) and PATs (G–I) of specific lineages, identified by numbers (see Table 2 for correspondence of lineage name and number). In panel G, similar to B″ above, PATs and SATs are co-labeled by *insc*-Gal4/BP104. All *z*-projections cover a brain slice of 12–15 μm thickness, located at the same antero-posterior level. SATs/PATs can be identified on the basis of their characteristic points of entry and trajectory; note, for example, the crescent-shaped tract formed by the DPLal1-3 lineages (#33∗ in D–I), the entry of DPLam (#36) medially adjacent to DPLal, the convergence of BLAd (#68∗) latero-ventral of DPLal, the convergence of BLAv (#73–75) ventral of BLAd, the convergence of BAlp1-3 (#6-8) ventro-medially of BLAv, the long descending tract, passing over peduncle, formed by DALcm1-2 (#20∗) and DALd (#22), or the ventral longitudinal tract formed by BAmv1-2 (#15∗). Red arrows in (E) point at the two separable SATs of BAmv1 and BAmv2 in 72 h brain; the corresponding primary tracts form a single bundle in 12 h brain (red arrowhead in I). White arrows in panels D–I indicate brain midline. Bars: 50 μm (B–G); 20 μm (H, I).

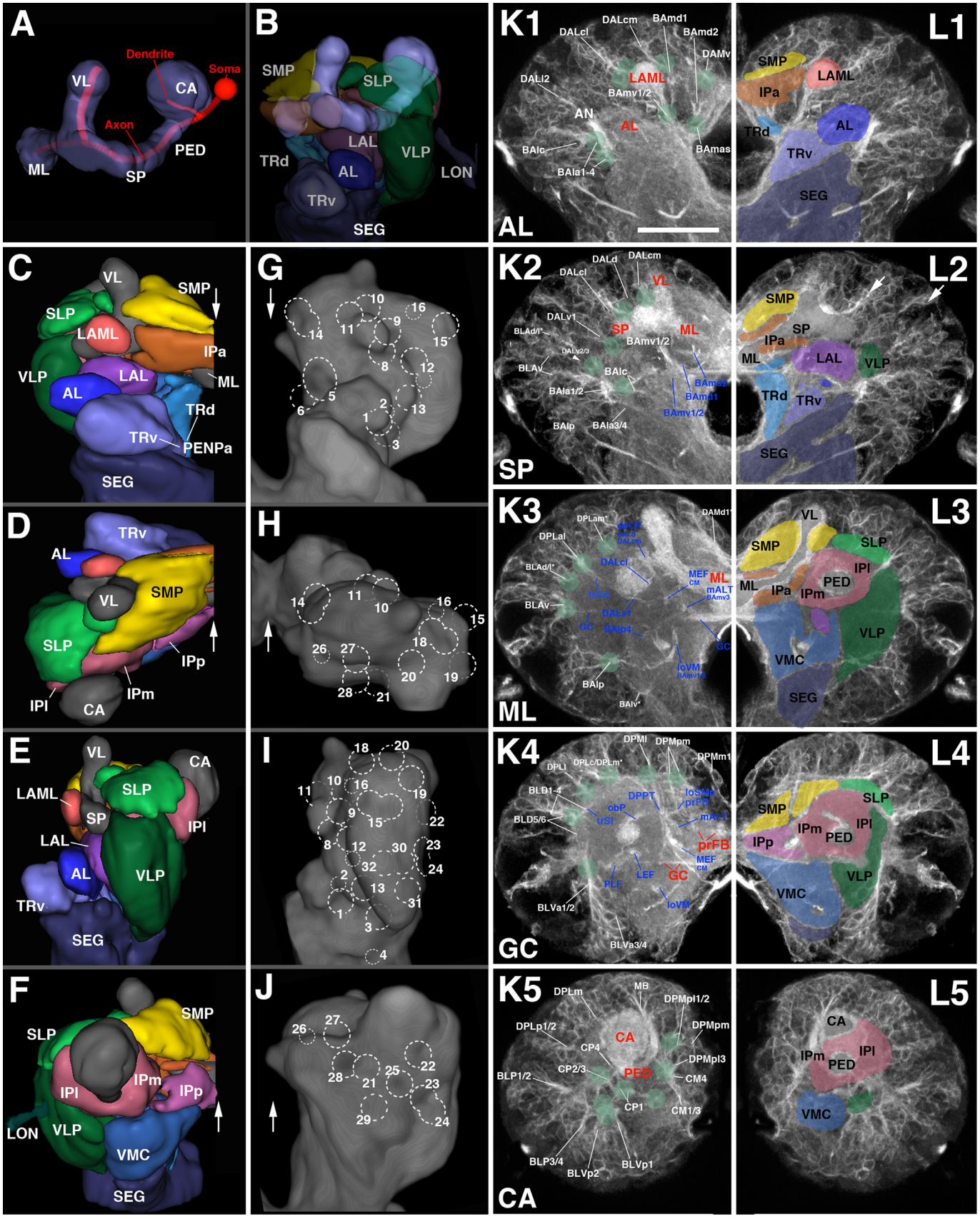
A
Dendrite
Soma
VL
CA
Axon
PED
ML
SP
B
SMP
SLP
LAL
VLP
TRd
AL
LON
TRv
SEG
C
VL
SMP
SLP
LAML
IPa
VLP
LAL
ML
AL
TRd
TRv
PENPa
SEG
D
TRv
AL
VL
SMP
SLP
IPp
IPm
IPl
CA
E
VL
CA
LAML
SLP
SP
IPl
LAL
AL
VLP
TRv
SEG
F
SMP
SLP
IPl
IPm
IPp
LON
VLP
VMC
SEG
G
H
I
J
K1
DALcm
BAmd1
DALcl
BAmd2
DAMv
DALl2
LAML
BAmv1/2
AN
AL
BAlc
BAmas
BAla1-4
AL
L1
SMP
LAML
IPa
TRd
AL
TRv
SEG
K2
DALd
DALcm
DALcl
VL
DALv1
BLAd/l*
SP
ML
BAmv1/2
DALv2/3
BLAv
BAlc
BAla1/2
BAmd2
BAmd1
BAmv1/2
BAlp
BAla3/4
SP
L2
SMP
SP
IPa
ML
LAL
VLP
TRd
TRv
SEG
K3
DPLam*
DAMd1
DPLal
BLAd/l*
DALcl
MEF
ML
mALT
BAmv3
BLAv
lrSA
DALv1
GC
BAlp4
loVM
BAmv1/2
BAlp
BAlv*
ML
L3
VL
SMP
SLP
IPl
ML
IPa
IPm
PED
VLP
VMC
SEG
K4
DPMl
DPMpm
DPMm1
DPLl
DPLc/DPLm*
BLD1-4
DPPT
loSMP
prFB
obP
BLD5/6
lrSI
mALT
prFB
MEF
LEF
GC
PLF
loVM
BLVa1/2
BLVa3/4
GC
L4
SMP
SLP
IPm
IPl
IPp
PED
VLP
VMC
K5
DPLm
MB
DPMpl1/2
DPLp1/2
DPMpm
CA
CP4
DPMpl3
BLP1/2
CP2/3
PED
CM4
CP1
CM1/3
BLP3/4
BLVp2
BLVp1
CA
L5
CA
IPm
IPl
PED
VMC

### 3.2. Reconstruction of primary axon tracts in the L1 larval brain

*Drosophila* brain lineages were initially identified and mapped for the late larval stage (L3), when each lineage forms a distinct SAT that can be visualized using global markers such as BP106 (Cardona et al., 2010a; Pereanu and Hartenstein, 2006). With only two exceptions all of these lineages were validated by MARCM clones in the adult brain (Kuert et al., 2014; Wong et al., 2013). Using the above described markers for SATs and PATs, we traced lineages backward in time from the late larval stage into the late first/early second instar, when secondary lineages are born (Fig. 1D–I; Supplementary Figs. S2 and S3; see also Lovick et al., 2015). Given that SATs project along the tracts formed earlier by the corresponding primary neurons, we could establish a map of primary axon tracts for the L1 larval brain ("L1 PAT map"). In the absence of specific markers, the map is of less resolution than the map of lineages and tracts in the late larva, because fiber bundles formed by pairs or small groups (3–4) of lineages have collapsed into one tract. Thus, as previously described, most lineages are arranged in pairs (e.g., BAmv1/2) or small groups of 3–4 (e.g., DPLal1-3; BLAd1-4) whose SATs enter and then extend through the neuropil in close apposition. In the late larva, when secondary neurons with their SATs have been added to each lineage, the SATs of these pairs or small groups can be separately followed from the cortex into the neuropil (see, for example, the two tracts formed by BAmv1/2, 15∗ shown by red arrows in Fig. 1E). In the L1 brain, at the level of primary lineages, the tracts have collapsed into one bundle (e.g., BAmv1/2 bundle indicated by red arrowhead in Fig. 1I). This decline in resolution aside, the primary axon tract map of the L1 brain reconstructed in this paper still represents a rich three-dimensional scaffold of structural landmarks around which neuroblasts and their progeny are grouped.

### 3.3. Neuropil compartments and long axon fascicles form a neuroanatomical framework for the lineage map

The brain neuropil has been described in terms of distinct compartments, domains of high synaptic density surrounded by bundles of long axons and glial processes that form visible boundaries (Pereanu et al., 2010). Compartments and selected fiber bundles forming compartment boundaries constitute a framework of landmarks of the developing *Drosphila* brain. The points of entry of lineage tracts, defined as the "entry portals" of the corresponding lineages (Lovick et al., 2013; Wong et al., 2013), as well as the fiber trajectories within the neuropil, can be described with respect to their invariant spatial relationship to compartment boundaries. We will therefore provide a brief review of the compartmental composition of the larval brain (for detail see legend of Fig. 2).

The most conspicuous compartment is the mushroom body (MB), which is formed by four lineages located at the posterior surface of the brain (Fig. 2A and B), and comprises the peduncle (PED), calyx (CA), spur (SP), vertical lobe (VL), and medial lobe (ML; Fig. 2A). Four compartments, the antennal lobe (AL), anterior peri-esophageal neuropil (PENPa), lateral appendix of the medial lobe (LAML), and anterior inferior protocerebrum (IPa), flank the MB lobes anteriorly (Fig. 2B, C, L1, and L2). [Note that we will in the following use the nomenclature that reflects the correspondence between larval and adult compartments; see Ito et al. (2014) and Pereanu et al. (2010). For correspondences between these terms and the nomenclature originally introduced for the larval brain in Younossi-Hartenstein et al. (2003) see Table 1.] The lateral

**Fig. 2.** Architecture of the first instar (L1) larval brain. (A and B) Digital 3D model of mushroom body, antero-lateral view. Mushroom body is rendered in blue gray (A and B; CA calyx; ML medial lobe; PED peduncle; SP spur; VL vertical lobe). In (A), an individual mushroom body neuron (Kenyon cell) is shown in red. In (B), neuropil compartments surrounding the mushroom body are shown in a semitransparent manner and in the same colors used in the following panels. (C–F) Digital 3D models of L1 brain hemispheres shown in different views (C: anterior; D: dorsal; E: lateral; F: posterior). Midline indicated by white arrow. Mushroom body rendered in gray, compartments in different colors. (G–J) Volume renderings of L1 brain neuropil labeled with anti-DN-cadherin, visualizing relief of neuropil surface. Except for I, each panel shows the contralateral brain hemisphere in the same view as 3D model to the left (G: anterior; H: dorsal; I: lateral; J: posterior). Numbered hatched circles indicate entry portals of lineage associated tracts. (K1–5, L1–5) *z*-Projections of frontal confocal sections of a L1 brain hemisphere labeled with anti-Neuroglian (BP104), illustrating lineages and lineage-associated fiber bundles (K1–5) in the context of larval brain neuropil compartments (L1–L5). Each *z*-projection represents a brain slice of approximately 8–10 μm thickness. *z*-Projections are presented in anterior (K1/L1) to posterior (K5/L5) order. Details of the anatomy of the mushroom body and surrounding structures present distinct "hallmarks" for a *z*-projection taken at a specific antero-posterior level (appear in red in K1–K5). These hallmarks are used in this and all following figures to define and name the antero-posterior level represented in the corresponding *z*-projection. The anterior level ("AL"; K1, L1) includes the neuropil anterior of the MB lobes, notably the antennal lobe (AL) and lateral appendix of the medial lobe (LAML); the second level ("SP"; K2, L2) is defined by the mushroom body spur (SP) and junction between vertical lobe (VL) and medial lobe (ML); the third slice ("ML"; K3, L3) contains the distal tips of the ML. The fourth level ("GC"; K4, L4) is defined by the posterior commissures, notably the great commissure (GC) and the primordium of the fan-shaped body (prFB). The posterior level ("CA"; K5, L5) shows the junction between the peduncle (PED) and calyx (CA). In panels K1–K5, lineages and neuropil fiber tracts are annotated with white lettering and blue lettering, respectively. White arrows in (L2) point at two examples of clusters of primary neurons that express higher levels of BP104 than surrounding cells. For additional information on lineages and fiber tracts they associate with, see Table 2. In panels L1–L5, which show the opposite hemisphere, compartments are rendered in different colors, following the color scheme used in panels B–F. For abbreviations of fiber tracts and compartments, see Table 1. Bar: 20 μm (for all panels).

Quick guide to neuropil compartments:

*Anterior compartments:* The PENPa represents the neuropil domain flanking the esophagus. It is subdivided into a ventral domain (TRv), which appears as the anteriorly directed tip of the subesophageal ganglion (SEG; C), and a dorsal domain (TRd). Both of these subdivisions receive input from the mouth cavity and foregut via the pharyngeal nerve (Rajashekhar and Singh, 1994); in view of its sensory input and internal lineage composition (discussed in detail in Kuert et al., in preparation), the PENPa domain corresponds to the tritocerebrum defined in adult flies (Rajashekhar and Singh, 1994) and other insects. The antennal nerve, carrying olfactory stimuli, defines the AL compartment, located laterally of the PENPa (panels C, L1). The LAML (Selcho et al., 2009), which has no counterpart in the adult brain, is a hemispherical structure capping the spur of the mushroom body (panels C, L1). Further medially, the IPa forms a cuff-shaped compartment that surrounds the medial lobe of the mushroom body (panels C, L1, and L2).

*Ventral compartments:* The LAL is located ventrally of the MB medial lobe and spur, and dorso-posteriorly of the antennal lobe and periesophageal neuropil (panels B, C, E, L2). A vertically-oriented gap in the ventral brain neuropil defines the boundary between the LAL and laterally adjacent VLP (panels C, G) and, further posteriorly, between the VLP and VMC (see Supplementary Fig. S4B and C).

*Inferior protocerebrum*: formed by compartments surrounding the lobes and peduncle of the mushroom body. Posterior to the anteriorly located IPa (flanking the medial lobe; see above) is the medial inferior protocerebrum (IPm). The IPm is separated from the postero-medially adjacent posterior inferior protocerebrum (IPp) by a robust mass of fibers/glia formed by the antennal lobe tract (ALT) and medial equatorial fascicle (MEF; panels K4, L4). A virtual vertical plane through the peduncle separates the IPm from the lateral inferior protocerebrum (IPl; L3–L5). Borders between IPm/l and ventrally adjacent VMC and VLP, respectively, are defined by several primary axon tracts (e.g., PLF; panels K4, L4; see also Supplementary Fig. S4H).

*Superior protocerebrum:* The superior medial protocerebrum (SMP) lies dorsal of the IPa and is bounded medially by the vertical lobe of the mushroom body (VL; panels C, D, F, L2, L3). Posterior of the vertical lobe, axon bundles of the DPLc lineages (see below) separate the SMP from the laterally adjacent superior lateral protocerebrum (SLP; panels K4, L4). Several longitudinally and transversally oriented fiber bundles (longitudinal superior medial and superior lateral fascicles (loSM, loSL); transverse superior fascicles (trSA/I/P); see below) delineate the border between the superior and inferior protocerebral compartments (panels K3-K4, L3, L4; and Supplementary Fig. S4G and H).

accessory lobe (LAL), ventromedial cerebrum (VMC), and ventrolateral protocerebrum (VLP) represent the ventral compartments of the L1 brain (Figs. 2B–G and S4A–C). The neuropil domains surrounding the peduncle and medial lobe of the mushroom body are termed "inferior protocerebrum" or "clasp" (Ito et al., 2014; Pereanu et al., 2010; IPa, l, m, p; Figs. 2F, L3–L5 and S4B, C, F). The superior protocerebrum (SP), comprising a superior lateral (SLP) and superior medial (SMP) domain, forms the dorsal compartments of the brain (Figs. 2C–F, K3, K4, L2, L3 and S4G, H).

A system of longitudinal fascicles interconnects neuropil domains of the insect ventral nerve cord (VNC) at different anteroposterior levels (Power, 1948; Tyrer and Gregory, 1982). These fascicles, which in *Drosophila* are commonly marked by the expression of the adhesion protein Fasciclin II (FasII; Grenningloh et al., 1991), include a regularly spaced medial, intermediate, and lateral system (Fig. 3). Anti-Neuroglian, which more globally labels primary axons, also faintly visualizes these fiber systems (Fig. 3A–C). Medial and lateral tracts each have a dorsal (DMT, DLT) and ventral component (VMT, VLT), respectively. The intermediate fascicle has several components extending along the center of the VNC neuropil (CIT1-3) (Nassif et al., 2003; Landgraf et al., 2003b). Anteriorly, the long axon tracts of the ventral nerve cord anastomose with each other and continue towards the brain (Nassif et al., 2003). They form three main bundles, termed medial cervical tract (MCT), lateral cervical tract (LCT), and posterior cervical tract (PCT). Each of these fiber systems, which carry ascending and descending axons connecting brain and VNC, splits up into smaller branches shown in Fig. 3B–F. A small number of these FasII-positive connectives associate with discrete primary lineages, which contain FasII-positive neurons (for specific detail, see below).

### 3.4. Synopsis of neuro-anatomical features of the early larval brain provided by lineage-associated tracts

We will in the following sections present detailed descriptions of all of the lineage-associated PATs labeled by the global marker anti-Neuroglian, including their position of entry into the neuropil (entry portals) and trajectory within the neuropil. For didactic reasons, we will proceed by breaking down lineages into their topologically defined groups. Before going into this detail, we present first a summary of our findings in Fig. 4 and Table 2. Overall, we can distinguish 68 discrete fiber bundles that enter the brain. As indicated in the second column (B) of Table 2, these

**Table 1**
Abbreviations for fiber tracts and neuropil compartments of the *Drosophila* early larval brain.

| Fiber tracts | Abbr. | Fiber tracts (cont'd.) | Abbr. | Compartments | Abbr. |
|---|---|---|---|---|---|
| Anterior-dorsal commissure | ADC | Supraellipsoid body commissure | SEC | Lateral appendix of medial lobe | LAML |
| Antennal lobe commissure | ALC | Subellipsoid body commissure | SuEC | Antennal lobe | AL |
| Antennal lobe tract | ALT | Transverse superior anterior fasicle | trSA | Anterior optic tubercle | AOTU (CPLd[a]) |
| Antennal nerve | AN | Intermediate superior transverse fascicle | trSI | Inner optic anlage | IOA |
| Basolateral protocerebral tract | BLPT | Transverse superior posterior fascicle | trSP | Inferior protocerebrum | IP |
| Basomedial protocerebral tract | BMPT | Medial trSP | trSPm | Anterior inferior protocerebrum | IPa (CA[a]) |
| Central intermediate tract | CIT1-3 | Ventrolateral longitudinal tract | VLT | Lateral inferior protocerebrum | IPl (CPL[a]) |
| Dorsal CIT | CITd | Ventromedial longitudinal tract | VMT | Medial inferior protocerebrum | IPm (CPM[a]) |
| Ventral CIT | CITv | Ventral nerve cord | VNC | Posterior inferior protocerebrum | IPp (CPM[a]) |
| Descending bundle | deCP | Vertical tract of the SLP | vSLPT | Lateral accessory lobe | LAL (BC[a]) |
| Dorsolateral longitudinal tract | DLT | | | Lateral appendix of the medial lobe | LAML |
| Dorsomedial longitudinal tract | DMT | | | Lateral horn | LH (CPLd[a]) |
| Dorso-posterior protocerebral tract | DPPT | | | Larval optic neuropil | LON |
| Frontomedial commissure | FrMC | | | Mushroom body | MB |
| Great commissure | GC | | | Calyx of MB | CA |
| Commissure of the lateral accessory lobe | LALC | | | Medial lobe of MB | ML |
| Lateral cervical tract | LCT | | | Peduncle of MB | PED |
| Lateral equatorial fascicle | LEF | | | Spur of MB | SP |
| Anterior LEF | LEFa | | | Vertical lobe of MB | VL |
| Posterior LEF | LEFp | | | Anterior periesophageal neuropil | PENPa (Bcv[a]) |
| Longitudinal superior lateral fascicle | loSL | | | Dorsal PENPa (tritocerebrum) | TRd |
| Longitudinal superior medial fascicle | loSM | | | Ventral PENPa (tritocerebrum) | TRv |
| Anterior loSM | loSMa | | | Primordium of the fan-shaped body | prFB |
| Posterior loSM | loSMp | | | Subesophageal ganglion | SEG |
| Intermediate longitudinal ventral fascicle | loVI | | | Superior lateral protocerebrum | SLP (CPLd[a]) |
| Lateral longitudinal ventral fascicle | loVL | | | Lateral SLP | SLPl |
| Medial longitudinal ventral fascicle | loVM | | | Posterior SLP | SLPp |
| Posterior-lateral longitudinal ventral fascicle | loVP | | | Latero-posterior SLP | SLPpl |
| Median bundle | MBDL | | | Medio-posterior SLP | SLPpm |
| Medical cervical tract | MCT | | | Superior medial protocerebrum | SMP (DA/DP[a]) |
| Medial equatorial fascicle | MEF | | | Superior protocerebrum | SP |
| Anterior MEF | MEFa | | | Ventrolateral protocerebrum | VLP (BPL[a]) |
| Medio-lateral antennal lobe tract | mlALT | | | Ventromedial cerebrum | VMC (BPM[a]) |
| Second nerve of corpora cardiaca | NCC2 | | | | |
| Oblique posterior fascicle | obP | | | | |
| Posterior cervical tract | PCT | | | | |
| Posterior lateral fascicle | PLF | | | | |
| Dorsal PLF | PLFd | | | | |
| Ventral PLF | PLFv | | | | |
| Commissure of the PLP | PLPC | | | | |
| Pharyngeal nerve | PN | | | | |
| Superior arch commissure | SAC | | | | |

*Column A*: List of fiber tracts and associated abbreviations.
*Column B*: List of larval neuropil compartments and associated abbreviations.

[a] Indicates older version larval compartment nomenclature as described in Younossi-Hartenstein et al. (2003).

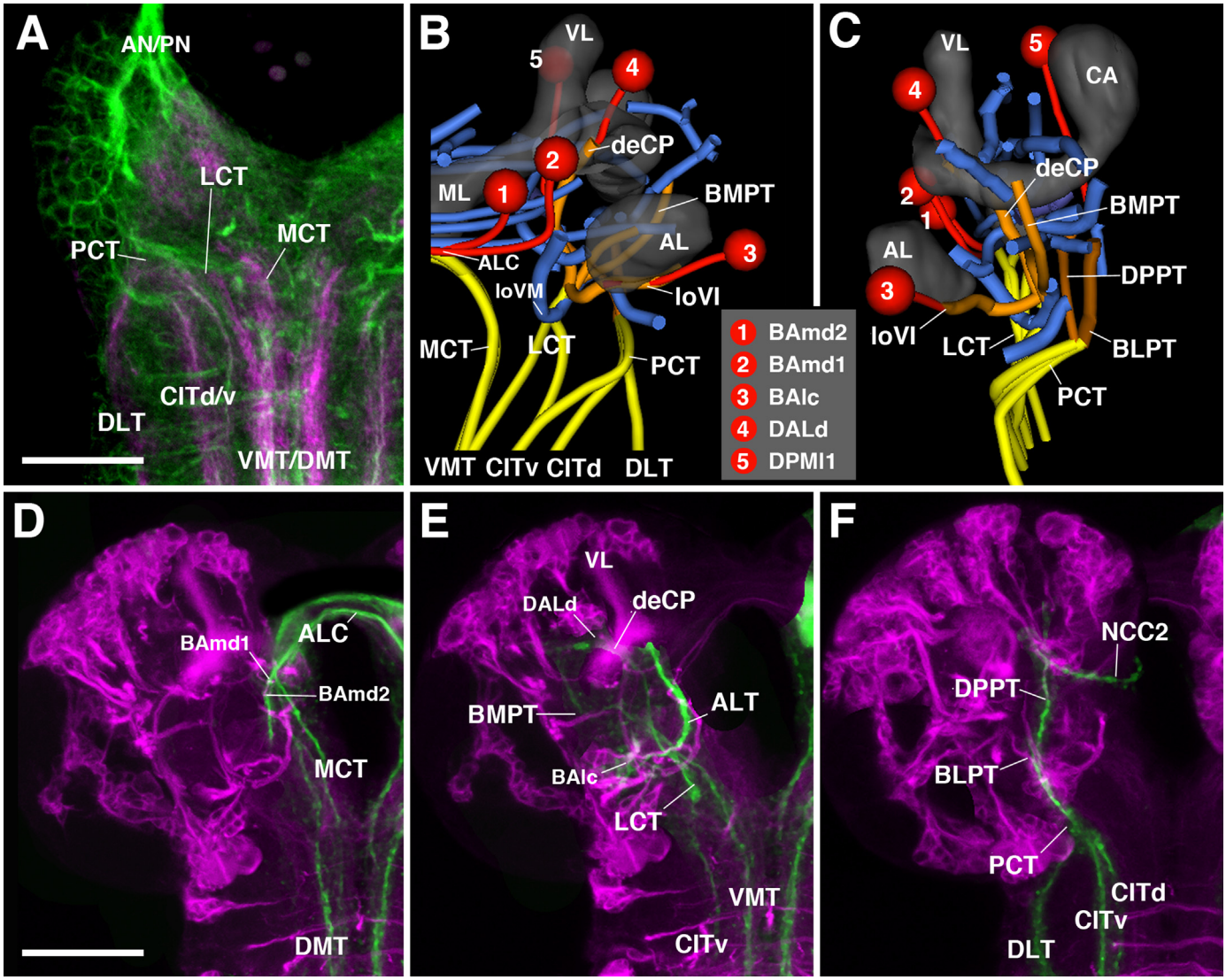


**Fig. 3.** Association of brain lineages and tracts with FasII-positive fiber bundles. (A) *z*-Projection of horizontal confocal sections of L1 larval anterior ventral nerve cord and basal brain, labeled with FasII-Gal4 (magenta) and anti-Neuroglian (BP104, green). FasII is expressed on each side in three pairs of long fiber tracts (CITd/v dorsal and ventral component of central intermediate tract; DLT dorsal lateral tract; VMT/DMT ventral and dorsal medial tract). These tracts anastomose in the anterior nerve cord (subesophageal ganglion, SEG) and continue as the cervical tracts into the basal brain (LCT lateral cervical tract; MCT medial cervical tract; PCT posterior cervical tract). (B and C) 3D digital model of FasII-positive tracts (yellow, orange) in spatial relationship to central brain neuropil tracts (blue), selected lineages (red) and central brain neuropil compartments.Anterior view (B) and lateral view (C). (D–F) *z*-Projections of frontal confocal section of third instar brain labeled with *insc*-Gal4, UAS-chRFP-Tub (magenta; labels secondary lineages) and anti-FasII (green). The three cervical tracts and their projections in the brain are shown separately [D: medial cervical tract (MCT); E: lateral cervical tract (LCT); F: posterior cervical tract (PCT)]. For abbreviations of compartments and tracts see Table 1. Bars: 20 μm (A); 50 μm (D–F).

bundles can correspond to: one lineage (e.g., BAmd1), small sets of adjacent lineages (e.g., BAla3/BAla4), single hemi/sublineages (e.g., DPMpm1a), or two hemilineages of neighboring lineages (e.g., DALcm1m/DALcm2m). Within the neuropil, these fiber bundles form larger fascicles that can be classified, by their main orientation according to body axis, into longitudinal, transverse, and vertical (ascending/descending) fascicles. These fascicles could be identified with their counterparts described for the brain at later stages of development (late larva to adult; Pereanu et al., 2010; Lovick et al., 2013). Table 2 and Fig. 4 represent these fascicles, color coded and assigned to the lineages that contribute to them. The basal-anterior (BA) lineages, according to previous studies (Kuert et al., 2012; Kumar et al., 2009), belong predominantly to the deuterocerebrum; two lineages, BAlv and BAlp4, in addition to three other subesophageal lineages not considered here, are positive for the Hox gene *labial*, a marker of the tritocerebrum. BA lineages form a set of longitudinal fascicles (loVM, loVI, loVL; dark blue), as well as two ascending fiber systems (red): the antennal lobe tract (ALT; formed by BAla1, BAlc, BAmv3, BAlp4) connecting the antennal lobe and neighboring territories to the dorso-posterior protocerebrum, and (part of) the median bundle (MBDL, dark red; formed by BAmas1/2) that leads from the PENPa to the dorso-anterior protocerebrum (Fig. 4A top, B, F, D, H). Lineages of the DAL and DAM group form the anterior protocerebrum (note that “anterior,” relative to the body axis, corresponds to “ventral” relative to the neuraxis; see Ito et al., 2014). DAL lineages, in addition to the dorsal most BA lineages (BAmd1/BAmd2), mainly form systems of transverse fiber bundles and commissures flanking the lobes of the mushroom body and the surrounding IPa compartment (ALC, FrMC, SuEC; green in Fig. 4A top, B, F). The lineage DALd, and part of DALcm1/2, form the major descending bundle (deCP; orange in Fig. 4A) projecting from the protocerebrum to the ventral brain and SEG (Fig. 4A, B, F, G). DAM lineages enter the anterior part of the SMP (superior medial protocerebrum) compartment and form commissural (ADC, green) as well as longitudinal fibers (loSMa; blue in Fig. 4A, B, F, H).

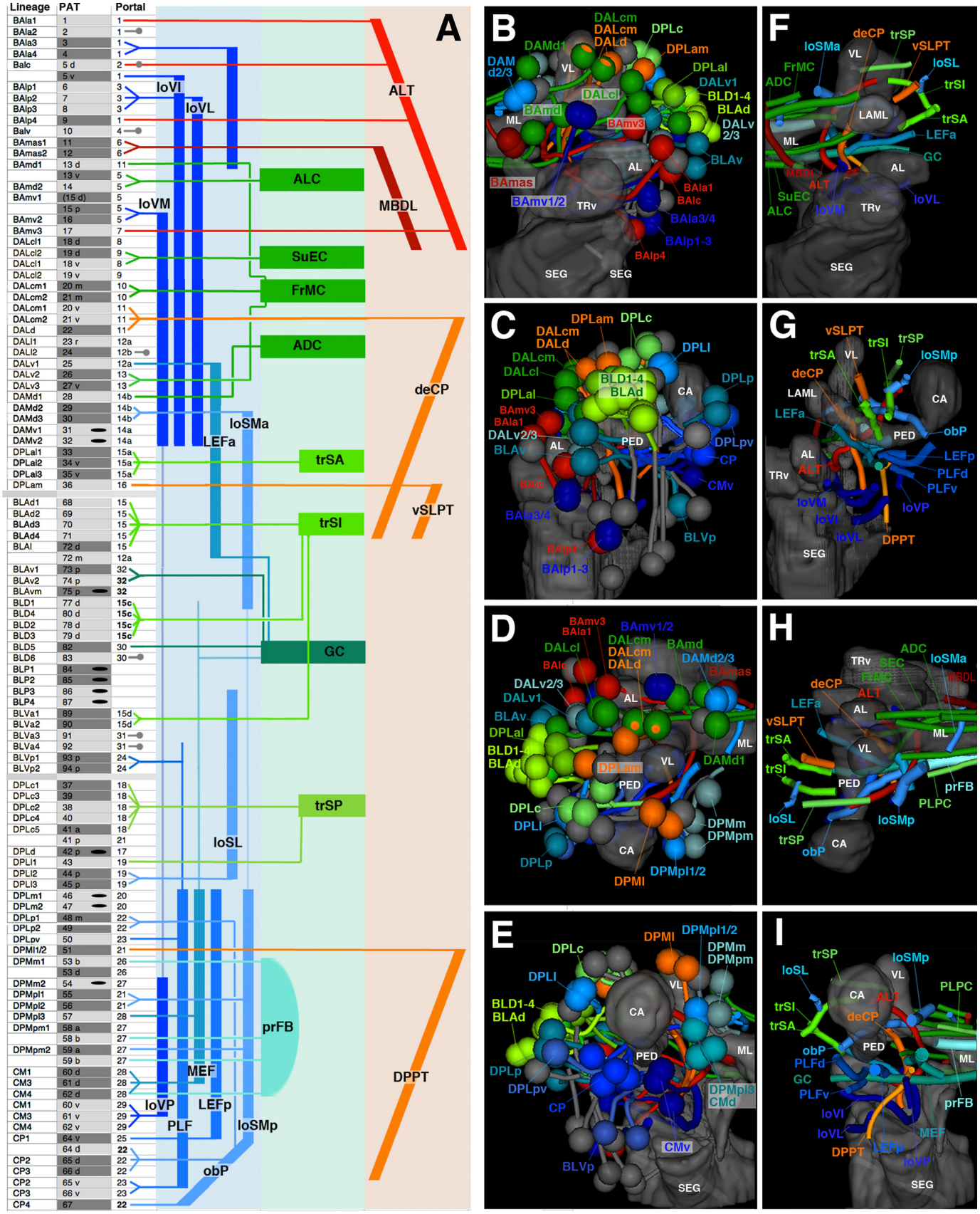


**Fig. 4.** Synopsis of lineages and neuropil tracts. (A) List of lineages (first column), associated PAT tracts (second column), and neuropil entry portals (third column). Neuropil fiber tracts are represented by colored bars at the right of panels; longitudinal tracts are in blue, transverse tracts/commissures in green, ascending and descending tracts in red and orange, respectively. Lines connect individual lineages (left) with the appropriate neuropil tracts (right). Lineages that project locally (according to specific labeling) are indicated by short gray lines and circles (third column); lineages for which no clear information exists are indicated by black oval in second column. (B–I) Digital 3D models of lineages (B–E) and tracts (F–I). Mushroom body and ventral brain neuropil compartments are shown semi-transparently for reference. Anterior view (B, F; medial to the left), lateral view (C, G; anterior to the left); dorsal view (D, H; medial to the right); posterior view (E, I; medial to the right). Coloring of lineages reflects their projection along longitudinal fiber system (blue), transverse system (green), or ascending/descending system (red or orange, respectively). For abbreviations of fiber tracts and compartments see Table 1.

**Table 2**
Lineages of the *Drosophila* early larval brain.

| A Lineage | B # | C Gal4 | D Portal | E # | F Tract |
|---|---|---|---|---|---|
| BAla1 | 1 | Per[a] | AL vl | 1 | mlALT |
| BAla2 | 2 | OK371[b] | AL vl | 1 | |
| BAla3 | 3 | En[a] | AL vl | 1 | |
| BAla4 | 4 | | AL vl | 1 | |
| BAlc | 5 d | GH146[a] R75C05(s)[c] | AL l | 2 | mALT |
| | 5 v | | AL vl | 1 | loVl > GC |
| BAlp1 | 6 | | VLP vm | 3 | |
| BAlp2 | 7 | | VLP vm | 3 | loVL |
| BAlp3 | 8 | | VLP vm | 3 | loVL > vP |
| BAlp4 | 9 | R46C11[c] | AL vl | 1 | mALT |
| BAlv | 10 | | VLCi v | 4 | 0 |
| BAmas1 | 11 | | AL vm | 6 | MBDL |
| BAmas2 | 12 | Ems[d] | AL vm | 6 | MBDL |
| BAmd1 | 13 d | | VL vm | 11 | FrMC |
| | 13 v | R58F02(v)[c] | AL v | 5 | ALC |
| BAmd2 | 14 | R34C01, R58F02(v)[c] | AL v | 5 | ALC |
| BAmv1 | 15 p | Per[a] | AL v | 5 | loVM |
| BAmv2 | 16 | R33C10, R76B11[c] | AL v | 5 | loVM |
| BAmv3 | 17 | GH146[a], R74A02, R46C11[c] | AL d | 7 | mALT |
| DALcl1 | 18 d | STAT[a], R82E10[c] | SP d | 9 | |
| DALcl2 | 19 d | | SP d | 9 | SuEC |
| DALcl1 | 18 v | | SP v | 8 | SuEC |
| DALcl2 | 19 v | | SP v | 8 | LEa |
| DALcm1 | 20 m | | VL vm | 11 | FrMC |
| DALcm2 | 21 m | | VL vm | 11 | FrMC |
| DALcm1 | 20 v | | VL vl | 10 | deCP |
| DALcm2 | 21 v | | VL vl | 10 | deCP |
| DALd | 22 | | VL vl | 10 | deCP |
| DALl1 | 23 r | R46C11[c] | VLP dm | 12 | trSIi? |
| DALl2 | 24 | | VLP dm | 12 | |
| DALv1 | 25 | R58F02[c] | VLP dm | 12 | LEFa > GC |
| DALv2 | 26 | Per[a], R48B12[c] | LAL v | 13 | LEa |
| DALv3 | 27 | En[a] | LAL v | 13 | |
| DAMd1 | 28 | | VL dm | 14 | ADC |
| DAMd2 | 29 | | VL dm | 14 | loSMa |
| DAMd3 | 30 | | VL dm | 14 | |
| DAMv1 | 31 | | VL dm | 14 | |
| DAMv2 | 32 | | | 14 | |
| DPLal1 | 33 | R36C09[c] | SLP l | 15 a | trSA |
| DPLal2 | 34 v | | SLP l | 15 a | trSA |
| DPLal3 | 35 v | | SLP l | 15 a | trSA |
| DPLam | 36 | En[a] | SLP a | 16 | vSLPT |
| DPLc1 | 37 | | SLP pm | 18 | trSPm |
| DPLc3 | 39 | | SLP pm | 18 | trSPm |
| DPLc2 | 38 | | SLP pm | 18 | |
| DPLc4 | 40 | | SLP pm | 18 | |
| DPLc5 | 41 a | | SLP pm | 18 | trSPm |
| | 41 p | | CA m | 21 | |
| DPLd | 42 | | VL dl | 17 | |
| DPLl1 | 43 | | SLP pl | 19 | trSPl |
| DPLl2 | 44 p | | SLP pl | 19 | loSLp |
| DPLl3 | 45 p | | SLP pl | 19 | loSLp |
| DPLm1 | 46 | | SLP p | 20 | 0 |
| DPLm2 | 47 | | SLP p | 20 | 0 |
| DPLp1 | 48 m | | CA l | 22 | obP > sPLPC |
| DPLp2 | 49 | | CA l | 22 | |
| DPLpv | 50 | | PLP ps | 23 | PLFdl |
| DPMl1 | 51 | | CA m | 21 | DPPT |
| DPMm1 | 53 b | 9D11, R13A10[c] | PB dm | | prFB |
| | 53 d | | PB dm | 26 | |
| DPMm2 | 54 | | PB dl | 27 | |
| DPMpl1 | 55 | | CA m | 21 | loSMp |
| DPMpl2 | 56 | | CA m | 21 | loSMp |
| DPMpl3 | 57 | | PB v | 28 | MEF > GC |
| DPMpm1 | 58 a | 9D11, R13A10[c] | PB dl | 27 | mALT |
| | 58 b | | PB dl | 27 | dlrFB |
| DPMpm2 | 59 a | 9D11, R13A10[c] | PB dl | 27 | loSMp |
| | 59 b | | PB dl | 27 | dlrFB |
| CM1 | 60 d | 9D11, R13A10[c] | PB v | 28 | MEF > LALC |
| CM3 | 61 d | 9D11, R13A10, R81B07(s)[c] | PB v | 28 | MEF |
| CM4 | 62 d | 9D11, R13A10, R81B07(s)[c] | PB v | 28 | MEF |
| CM1 | 60 v | | VMC po | 29 | loVP |
| CM3 | 61 v | | VMC po | 29 | loVP > (pPLPC) |
| CM4 | 62 v | | VMC po | 29 | loVP > pPLPC |
| (CM5) | 63 | | PB v | | |
| CP1 | 64 d | R34A04, R34G03, R76A10[c] | CA l | **22** | MBDLchi |
| | 64 v | | CA v | 25 | LEF |
| CP2 | 65 d | | CA l | 22 | obP > loSM |
| CP3 | 66 d | | CA l | 22 | obP > loSM |
| CP2 | 65 v | | PLP ps | 23 | PLF d |
| CP3 | 66 v | | PLP ps | 23 | PLF d |
| CP4 | 67 | | CA l | **22** | obP > loSM |
| BLAd1 | 68 | | SLP l | 15 a | trSI |
| BLAd2 | 69 | | SLP l | 15 a | trSI |
| BLAd3 | 70 | | SLP l | 15 a | trSI |
| BLAd4 | 71 | | SLP l | 15 a | |
| BLAl | 72 d | | SLP l | 15 a | trSI |
| | 72 m | | VLP dm | 12 | |
| BLAv1 | 73 p | | VLP dl | 32 | GC |
| BLAv2 | 74 p | R46C11(s)[c] | VLP dl | 32 | GC |
| BLAvm | 75 p | R81B07, R46C11(s)[c] | VLP dl | 32 | |
| BLD1 | 77 d | | SLP l | 15 c | trSI |
| BLD4 | 80 d | | SLP l | 15 c | trSI |
| BLD2 | 78 d | | SLP l | 15 c | trSI |
| BLD3 | 79 d | | SLP l | 15 c | trSI |
| BLD5 | 82 | Ato[a], R67A11[c] | PLP l | 30 | GC |
| BLD6 | 83 | R67A11[c] | PLP l | 30 | |
| BLP1 | 84 | | | | |
| BLP2 | 85 | | | | |
| BLP3 | 86 | | | | |
| BLP4 | 87 | | | | |
| BLVa1 | 89 | So[a] | LH a | 15d | |
| BLVa2 | 90 | So[a] | LH a | 15d | |
| BLVa3 | 91 | R67A11[c] | VLP vli | 31 | |
| BLVa4 | 92 | R67A11[c] | VLP vli | 31 | |
| BLVp1 | 93 p | R75B09[c] | PLP pi | 24 | PLFv > GC |
| BLVp2 | 94 p | R75B09[c] | PLP pi | 24 | PLFv > SEC |

*Column A*: Lineage names based on topology (Pereanu and Hartenstein, 2006). Bracketing of CM5 indicates that no primary lineage tract could be identified for this lineage.
*Column B*: Number identifying lineage-associated tracts (PATs) in Fig. 1. In lineages with multiple hemilineage tracts or sublineage tracts, these are individually listed (e.g., dorsal hemilineage tract of BAlc is identified as "5d", ventral hemilineage tract as "5v"). Differential light and dark shading indicates lineage tracts that have merged into a single bundle; for example, a single PAT is formed by BAmv1 and BAmv2, or for the dorsal hemilineages 18d and 19d of DALcl1 and DALcl2, respectively.
*Column C*: Markers for lineages.
*Column D*: Entry portal of lineage-associated tracts. For abbreviations see Table 1.
*Column E*: Number identifying entry portals in Figs. 2, 5–10, and 12.
*Column F*: Neuropil fascicle joined by lineage-associated tracts. For abbreviations of fascicle names see Table 1.

[a] Reviewed in Spindler and Hartenstein (2010).
[b] Das et al. (2013).
[c] Jenett et al. (2012).
[d] Lichtneckert et al. (2007).

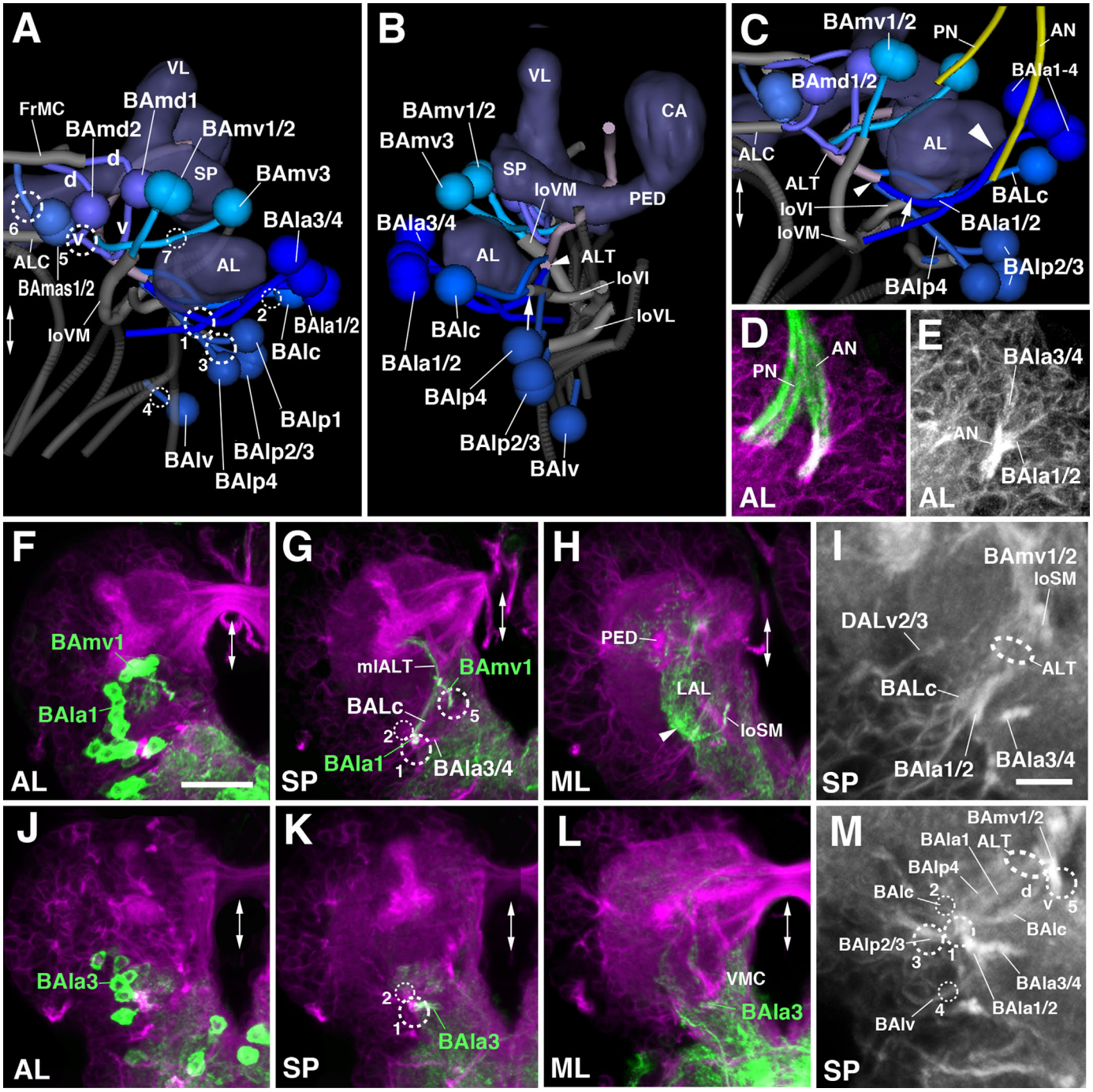


**Fig. 5.** Tracts associated with baso-anterior (BA) lineages. (A–C) Digital 3D models of BA lineages and tracts in a single L1 brain hemisphere. Anterior view (A), lateral view (B), ventro-anterior view (C). Centers of cell body clusters of lineages are depicted as spheres; lineage-associated axon tracts are shown as lines. Mushroom body and antennal lobe (blue-gray) and FasII-positive tracts (dark gray) are shown for reference. Fiber bundles of neuropil formed by BA lineage tracts are shown in light gray. Numbered hatched circles in (A) and other panels represent entry portals of lineage-associated tracts. "d" and "v" in (A) indicate dorsal and ventral hemilineage tracts of BAmd1 and BAmd2, respectively. Arrow in (B, C) points at entry of ventral hemilineage of BAlc into loVI tract; small arrowhead in (B, C) indicates convergence of tracts of BAla1, BAlc, and BAlp4 into the antennal lobe tract (ALT); large arrowhead in (C) points at close parallel entry of antennal nerve (AN) and tracts of BAla1-4. Double-headed arrow in (A, C) and all other panels indicates brain midline. (D–M) *z*-Projections of frontal confocal sections of a single L1 brain hemisphere. Antero-posterior levels shown by *z*-projections are indicated by letters (AL, SP, ML) at lower left corner (for definition of levels, see Fig. 2). Primary neurons and tracts are labeled by anti-Neuroglian (BP104; magenta in panels D, F–H, J–L; white in panels E, I, M). BP104-positive antennal nerve (AN) and pharyngeal nerve (PN) is highlighted in green in panel (D). Lineages BAmv1 and BAla1 are labeled by *per*-Gal4 > UAS-mcd8::GFP (green in F–H); BAla3 is labeled by *en*-Gal4 > UAS-mcd8::GFP (green in J–L). Panels (I) and (M) are high magnifications of central parts of (G) and (K), respectively. For abbreviations of compartments and fiber tracts see Table 1; for numbering of entry portals see Table 2. Bars: 10 μm (D, E, I, M); 20 μm (F–H, J–L).

DPL, BLA, and BLD lineages are associated with the dorsolateral protocerebrum. Many of these lineages converge on three transverse fiber systems (trSA: DPLal1-3; trSI: BLAd1-4, BLAl, BLD1-4; trSP: DPLc1-5, DPLl1) located in the superior lateral protocerebrum (SLP; light green in Fig. 4A center, B–I). BLAv1/2, as well as the posterior-lateral lineages BLVp1/2, forms the main ventral commissural system, the great commissure (GC, dark green; Fig. 4A center, F, I). The GC is also joined anteriorly by fibers of the DALv1 lineage and posteriorly by the CM group (see below; Fig. 4A, F, I). The pair DPLl2/3 forms a longitudinal fiber system

(loSL) in the SLP compartment.

DPM, CM, and CP lineages belong to the dorso-medial and posterior protocerebrums and mainly contribute to longitudinal fiber systems connecting the posterior protocerebrum with the anterior protocerebrum and deuterocerebrum. These include dorsal bundles (loSMp, formed by DPMpl1/2 and part of DPMpm2; Fig. 4A bottom, D, E, H, I), as well as ventral bundles. Most prominent among these is the medial equatorial fascicle (MEF), which forms a thick fascicle running medially of and parallel to the peduncle of the mushroom body. It is formed by dorsal components of the CM lineages, as well as DPMpl3 (Fig. 4A bottom, E, I). Further laterally are the lateral equatorial fascicle (LEFp, formed by CP1; Fig. 4A bottom, E, I), the postero-lateral fascicle (PLFd, formed by ventral components of CP lineages and DPLpv; PLFv, formed by BLVp1 and 2; Fig. 4A bottom, E, I), and the posterior ventral longitudinal fascicle (loVP, associated with ventral parts of the CM lineages; Fig. 4A bottom, E, I). Dorsal components of the CP group and DPLp1/2 form the conspicuous oblique posterior fascicle (obP), which crosses over the peduncle where it emerges from the calyx (Fig. 4A bottom, H, I); the obP turns anteriorly and joins the loSM bundle (Fig. 4A bottom, H). Two lineages, DPMl1/2, form a descending tract towards the SEG (DPPT; Fig. 4A bottom, E, I).

Compartments missing from the larval brain are those of the central complex, a prominent structure of the adult brain. The main (secondary) lineages contributing to the adult central complex are the four posterior lineages: DPMm1, DPMpm1/2, CM4 (fan-shaped body), and DALv2 (ellipsoid body). Several other lineages, including BAmv1 also contribute to the fan-shaped body (Wong et al., 2013). Based on a recent study (Riebli et al., 2013), primary neurons of DPMm1, DPMpm1/2, and CM4 form a commissural tract that, in the late larva, grows into a distinct fan-shaped body primordium. This commissural system is already visible in the early larval brain (Fig. 4A bottom, D, E, H, I; for details see below). No corresponding primordium of the ellipsoid body can be discerned; primary DALv2 neurons, whose secondary neurons form the ring-shaped volume of the adult ellipsoid body, project to the LAL and medial lobe of the mushroom body (see below). Midline-crossing fibers of DALv2/3 form a thin commissural system joining the FrMC commissure, which demarcates the location where the ellipsoid body will form during early metamorphosis (Fig. 4A center).

### 3.5. Antero-ventral lineages: the BA group

The BA cluster contains 17 lineages which form 11 bundles entering the anterior neuropil in the vicinity of the antennal lobe (AL). BAla1-4 form an antero-lateral BA subgroup with PATs that pass over the AL surface and converge at an entry point at the antero-lateral boundary of the AL, closely attached to the antennal nerve (entry portal AL vl, #1; Figs. 2G, I, K1, K2 and 5A–E). The BAla1/2 tract turns medially along the posterior boundary of the AL (Fig. 5B). The BAla2 lineage includes local interneurons (Das et al., 2013) that terminate within the AL. BAla1, marked by several known Gal4 driver lines, including *per*-Gal4 (Larsen et al., 2009; Fig. 5F–H), represents one of the four antennal lobe projection lineages. Its tract turns dorsally, forming part of the antennal lobe tract (ALT) that leaves the antennal lobe at its posterior boundary (Fig. 5B, G). The BAla1 tract soon exits the ALT towards laterally, approaches the peduncle, and terminates in the inferior protocerebrum surrounding the peduncle (Das et al., 2013; Fig. 5G, H). This peculiar pathway, which matches the corresponding BAla1 secondary axon tract in the adult brain, represents the mediolateral antennal lobe tract (mlALT; Das et al., 2013; Lovick et al.,2013). BAla3 is marked by *en*-Gal4 (Kumar et al., 2009; Fig. 5J–M). The BAla3/4 tract projects postero-medially, passes the large loVM bundle (see below) at its ventral surface, and branches in the ventromedial cerebrum (VMC; Fig. 5K, L).

BAlc, located posterior of the BAla1-4 cluster, enters the posterior AL at a position dorsal of BAla1/2 (entry portal AL l, #2; Figs. 2G, I, K1, K2 and 5B, I). Similar to the corresponding secondary tract in the late larva and adult, the BAlc tract bifurcates with one branch projecting dorso-medially and the other one ventro-medially (Fig. 2K2; arrow and arrowhead in Fig. 5B). The dorso-medial branch joins BAla1 towards the antennal lobe tract (ALT; arrowhead in Fig. 5B, C). Primary BAlc neurons with this dorsal trajectory were described as local antennal interneurons, as well as atypical projection neurons (Das et al., 2013). In the adult brain, the dorsal BAlc neurons form a hemilineage of uni-glomerular projection neurons (Lai et al., 2008). The ventral branch of BAlc, similar to its secondary counterpart at a later stage, converges upon the ventral longitudinal fiber system, forming the loVI (longitudinal ventral intermediate) fascicle, and projecting posteriorly towards the boundary between the ventromedial cerebrum and ventrolateral protocerebrum (VMC and VLP; arrow in Fig. 5B, C).

BAlp1-4 are located postero-ventrally of BAla1-4 (Figs. 2K2, K3 and 5A–C). BAlp1-3 converge upon a single, short, posteriorly-directed bundle entering the neuropil in the cleft between the lateral accessory lobe (LAL) and VLP compartments (entry portal VLP vm, #3). This trajectory corresponds to the longitudinal ventral lateral fascicle (loVL; Figs. 2K3 and 5A, C). BAlp4, marked by the Gal4 driver R46C11 (Table 2), contains atypical antennal lobe projection neurons (Das et al., 2013). The BAlp4 tract projects straight dorso-medially along the posterior boundary of the antennal lobe (AL), to join BAla1 and BAlc at the root of the antennal lobe tract (ALT; entry portal AL vl, #1; Fig. 5A–C, M). BAlv is located ventrally of the BAlp cluster and projects a short tract medially towards the boundary between VLP and subesophageal ganglion (SEG; entry portal VLCi v, #4; Figs. 2K3 and 5A, B, M). This entry point marks the position where a distinct compartment, the inferior ventrolateral cerebrum (VLC) which receives BAlv projections, will emerge (Lovick et al., 2013).

BAmas1/2 form a pair with a joined tract entering at the dorsomedial border of the anterior periesophageal ganglion (PENPa), medially of the antennal lobe (entry portal AL vm, #6), and projecting dorsally towards the superior medial protocerebrum (SMP; Figs. 2K1 and 5A). Located dorsolaterally of BAmas1/2 and medially of the lateral appendix of the medial lobe (LAML) are two lineages, BAmd1 and BAmd2. Both tracts project straight posteriorly towards the medial lobe of the mushroom body with the BAmd1 tracts entering slightly laterally of BAmd2 (entry portal ALv; #5; Figs. 2K1 and 5A). Similar to its secondary counterpart, BAmd1 bifurcates into a dorsal and ventral branch. The dorsal branch approaches the dorsal surface of the medial lobe (ML) and makes a sharp medial turn, joining the medially-directed tract of the DALcm1/2 lineage (see below). The joined tracts of the medial DALcm1/2 and dorsal BAmd1 cross the midline in the frontomedial commissure (FrMC; Fig. 5A). The ventral branch of BAmd1 approaches the ventral surface of the ML, turns medially, and crosses the midline as the antennal lobe commissure (ALC; Fig. 5A, C). The BAmd2 tract, entering medially and ventrally of BAmd1, also turns ventrally and then medially as part of the ALC (Fig. 5A, C). The ventral components of both BAmd1 and BAmd2 and their commissural tract express Fasciclin II (Fig. 3B–D). Markers for BAmd2 (e.g., R34C01-Gal4; Table 2) and GFP-labeled clones (Lovick et al., 2015) reveal that BAmd2 also possesses a second, dorsally-directed branch (not visible with anti-Neuroglian alone), similar to BAmd1 (Fig. 5A).

The last group of BA lineages, BAmv1-3, is located dorsally of the antennal lobe (AL; Fig. 5A–C). Together, the BAmv1/2 lineages form a common, thick tract that projects postero-ventrally and enters medially of the AL (entry portal AL v, #5; Figs. 2G, K1, K2

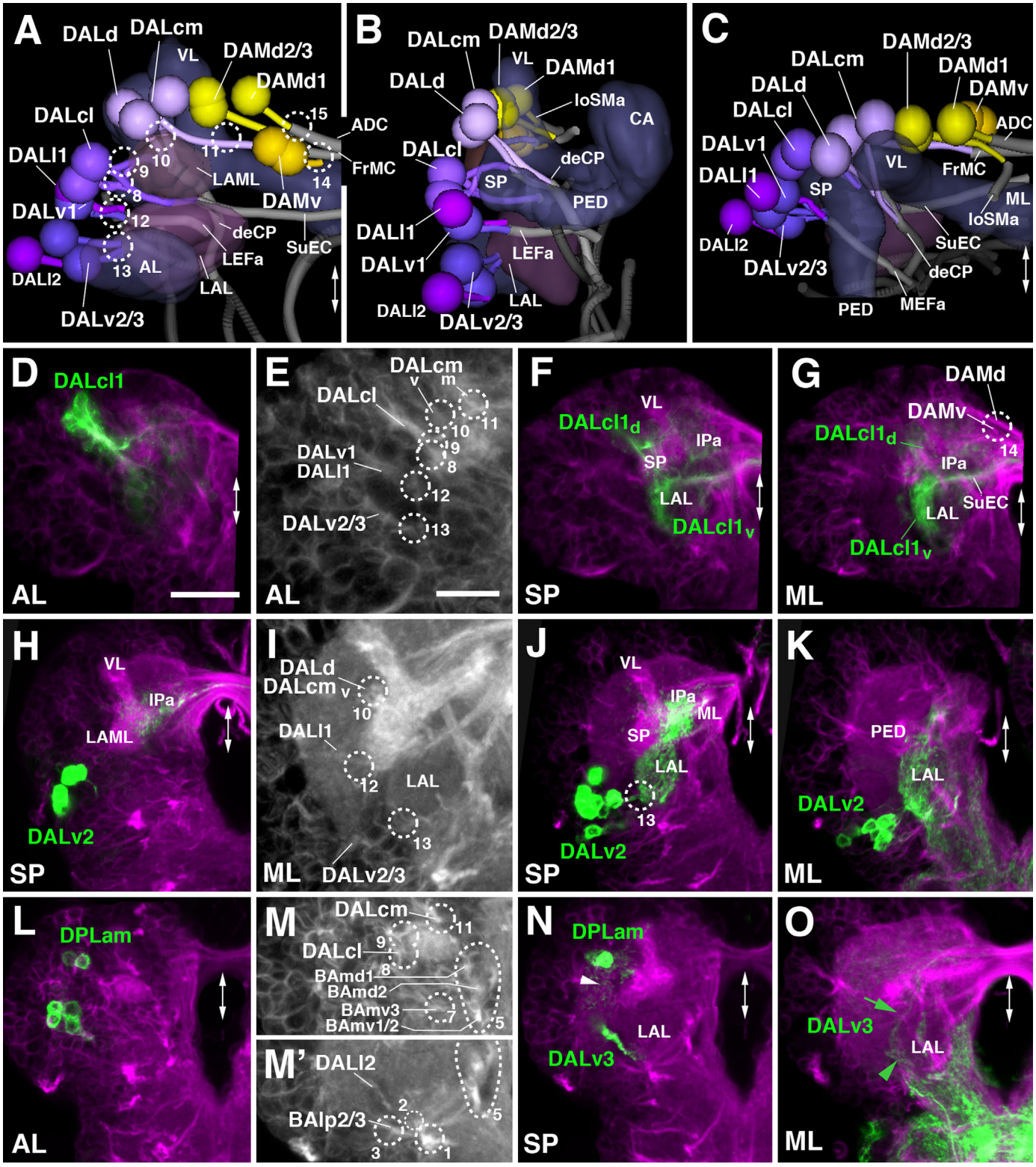


**Fig. 6.** Tracts associated with dorso-anterior lateral (DAL) and dorso-anterior medial (DAM) lineages. (A–C) Digital 3D models of DAL and DAM lineages and tracts in a single L1 brain hemisphere. Anterior view (A), lateral view (B), dorsal view (C). Aside from mushroom body and antennal lobe (blue-gray) and FasII-positive tracts (dark gray), the lateral accessory lobe (LAL) and lateral appendix of the medial lobe (LAML; both in magenta-gray) are shown for reference. Fiber bundles of neuropil formed by DAL lineage tracts are shown in light gray. Numbered hatched circles in (A) and other panels represent entry portals of lineage-associated tracts. Double-headed arrow in (A, C) and all other panels indicate brain midline. (D–O) *z*-Projections of frontal confocal sections of a single L1 brain hemisphere. Antero-posterior levels shown by *z*-projections are indicated by letters (AL, SP, ML) at lower left corner (for definition of levels, see Fig. 2). Primary neurons and tracts are labeled by anti-Neuroglian (BP104; magenta in panels D, F–H, J–L, N, O; white in panels E, I, M/M′). Lineage DALcl1 is labeled by R82E10-Gal4 > UAS-mcd8::GFP (green in D, F, G); DALv2 is labeled by *per*-Gal4 > UAS-mcd8::GFP (green in H, J, K); DALv3 and DPLam are labeled by *en*-Gal4 > UAS-mcd8::GFP (green in L, N, O). Panels (E), (I), (M) and (M′) are high magnifications of central parts of (D), (J) and (N), respectively. For abbreviations of compartments and fiber tracts see Table 1; for numbering of entry portals see Table 2. Bars: 20 μm (D, F, G, H, J–O); 10 μm (E, I).

and 5A). The tract, defining the medial longitudinal ventral fascicle (loVM), continues posteriorly, first along the boundary between the lateral accessory lobe (LAL) and anterior periesophageal ganglion (PENPa), then towards the boundary between the ventromedial cerebrum (VMC) and ventrolateral protocerebrum (VLP; Figs. 2K2, K3 and 5A–C, G). BAmv1 is marked by *per*-Gal4 (Larsen et al., 2009; Fig. 5F–I; Table 2), which reveals additional detail about the trajectory of this lineage. As described for the secondary BAmv1 lineage, primary BAmv1 gives off a crescent-shaped branch projecting dorsally along the lateral boundary of the LAL (Fig. 5H, arrowhead). BAmv3 constitutes the fourth antennal lobe projection neuron lineage; it contains all of the 20 or so projection neurons connecting the larval AL to the calyx and lateral horn (Das et al., 2013; Ramaekers et al., 2005). BAmv3 can be marked by several reporter lines, among them GH146-Gal4 (Stocker et al., 1997; Table 2). The BAmv3 tract (which is difficult to discern solely by anti-Neuroglian) enters the AL from a dorso-medial position, projecting medially right in front of the downward path of the ventral BAmd1 tract, and then turning posteriorly to join BAla1/BAlc/BAlp at the root of the antennal lobe tract (ALT; entry portal AL d, #7; Fig. 5A–C).

### 3.6. Antero-dorsal lineages: DAL and DAM

The DAL group possesses 10 lineages located anterior and lateral of the spur (SP) and vertical lobe (VL) of the mushroom body (Fig. 6A–C). DALcl1/2 forms a paired cluster which flanks the SP and emits a dorsal and a ventral tract (Figs. 2K1, K2 and 6A, B, D–G). DALcl1 is marked by the expression of R82E10-Gal4 (Table 2; Fig. 6D–G). The ventral tracts of DALcl1/2 project medially, passing the lateral appendix of the medial lobe (LAML) and entering medially of this compartment via the portal SPv (#8; Fig. 6A, E, M) As shown by marker R82E10, the ventral tract of DALcl1 continues medially and crosses the midline in a commissure that we interpret as the forerunner of the adult subellipsoid commissure (SuEC; Fig. 6A, F, G), as defined by the secondary DALcl1 tract (Lovick et al., 2013). The dorsal DALcl1/2 tract extends posteriorly and medially, crosses the peduncle at its dorsal surface, then turns ventrally (entry portal SP d, #9; Fig. 6A, E, M). These trajectories of DALcl1/2 primary axons resembles the pattern of secondary DALcl1/2 tracts (Lovick et al., 2013). Terminal arborizations of the dorsal DALcl1 tract (labeled by R82E10-Gal4) fill the anterior and medial inferior protocerebrums (IPa, IPm), posterior to the elbow formed by the lobes of the mushroom body (Fig. 6F, G); branching of the ventral tract occurs in the LAL (Fig. 6F, G).

DALcm1/2 and DALd are located medially of DALcl1/2, flanking the antero-lateral surface of the vertical lobe (VL; Figs. 2K1, K2 and 6A–C). The DALcm1/2 lineages form a cluster that produces a medial tract and a ventral tract. The medially-directed tract passes in front of the VL and is directed towards the midline; its crossing defines the forerunner of the frontomedial commissure (FrMC; entry portal VL vm, #11; Fig. 6A, B, E, I). The posterior tract curves around the lateral and posterior surface of the VL and then turns ventrally, joining the single tract of DALd which forms the descending deCP tract (entry portal VL vl, #10; Figs. 2K2 and 6A, B, E, I).

Three DALv lineages are located ventrally of DALcl1/2 (Figs. 2K2 and 6A–C). The DALv1 tract projects postero-medially into the space in between the lateral accessory lobe (LAL), ventrolateral protocerebrum (VLP), and spur (SP; entry portal VLP dm, #12; Figs. 2K2, L2 and 6A, B, E, I). It is closely attached to the ventromedial surface of the peduncle and continues posteriorly towards the great commissure, defining the anterior LEF fascicle (LEFa; Figs. 2K2, K3 and 6B, C). DALv2/3 form a cluster ventral of DALv1 (arrowhead in Figs. 2K2 and 6A, H–K). DALv2 is marked by *per*-Gal4 (Spindler and Hartenstein, 2010, 2011) and *poxn*-Gal4 (Boll and Noll, 2002; Minocha, 2010); DALv3 by *en*-Gal4 (Kumar et al., 2009; Larsen et al., 2009; Fig. 6L, N, O). The DALv2/3 tracts, which express Neurotactin only faintly, approach the lateral surface of the LAL, where they form terminal arborizations (entry portal LAL v, #13; Fig. 6A, B, E, I, J). The DALv2 tract (labeled by specific markers) then turns dorso-medially and forms dense arborizations in the LAL and surrounding the medial lobe of the mushroom body (Fig. 6J, K). Some axons cross the midline with the FrMC commissure and terminate in the medial lobe of the contralateral hemisphere (not shown).

Two lineages, DALl1/2, form the DALl group among the secondary lineages, and are located laterally of DALv1-3 (Cardona et al., 2010a; Lovick et al., 2013). Secondary DALl2 axons enter the antero-medial surface of the ventrolateral protocerebrum (VLP) in a very short tract. A cluster of neurons, that we interpret as DALl2, with axons converging onto the medial VLP close to entry portal VLPdm (#12) is also apparent in the L1 brain (Fig. 6A–C). DALl1, whose secondary component has a highly characteristic trajectory along the lateral surface of the peduncle and then backward to the anterior anterior optic tubercle (Lovick et al., 2013) was difficult to follow backward to the L1 stage. A primary lineage closely associated with DALv1, its tract running parallel to the DALv1 tract, is the only candidate for the primary DALl1 (entry portal VLP dm, #12; Figs. 2J2 and 6A, B).

A group of five DAM lineages is located medially of the mushroom body vertical lobe (Figs. 2K1–K3 and 6A–C). The most ventral component, DAMv1/2, projects two adjacent, thin tracts posteriorly into the superior medial protocerebrum (SMP; entry portal VL dm, #14; Figs. 2K1 and 6A, G). The DAMd lineages are located dorso-posteriorly of DAMv and enter the neuropil through the VL dm entry portal (#14 in Figs. 2 and 6). A medial group of neurons, interpreted as DAMd1, has medially-directed axons which reach the dorsal midline, defining the anterior-dorsal commissure (ADC; Fig. 6A, C, G). Secondary neurons of DAMd2/3 project posteriorly, forming the anterior longitudinal superior medial fascicle (loSMa; Lovick et al., 2013). Fibers emitted from the primary DAMd2/3 cluster which follow a similar posterior route are only faintly visible in some preparations (indicated as “loSMa” in Fig. 6A–C).

### 3.7. Dorso-lateral lineages: the DPL group

DPL lineages are widely dispersed over the dorso-lateral surface of the superior protocerebrum. One can distinguish the following subgroups with characteristic tract entry points: an antero-lateral DPLal with an adjacent DPLam and a DPLd cluster; a postero-lateral DPLl cluster; a posterior DPLp cluster; a dorsal DPLc cluster; and a dorso-posterior DPLm cluster. The DPLal cluster, presumably formed by three lineages, DPLal1-3, enters the superior lateral protocerebrum laterally (SLP; entry portal SLP l, #15a; Figs. 2G–I, K3 and 7A) and projects a thick bundle, the transverse superior anterior fascicle (trSA), ventro-medially towards the peduncle (PED; Figs. 2K3 and 7A, D, H, L). The trSA tract demarcates the boundary between the SLP compartment (above) and ventrolateral protocerebrum (VLP; below). DPLam is marked by the expression of *en*-Gal4 (Kumar et al., 2009; Fig. 6L, N). The short DPLam tract enters the SLP compartment medially of the trSA (entry portal SLP a, #16; Figs. 2G–I, K3 and 7A, B) and forms terminal arborizations in the SLP and the lateral inferior protocerebrum (IPl; Fig. 6N, arrowhead).

The DPLl group, which consists of three uniquely identifiable secondary lineages (DPLl1-3), is located posterior of DPLal. It forms a short tract entering the superior lateral protocerebrum (SLP) compartment latero-posteriorly (entry portal SLP pl, #19; Figs. 2H, I, K4 and 7B, C) and projects anteriorly, forming the longitudinal superior lateral fascicle (loSL; Figs. 2K4 and 7B, C, G, K, O). Even

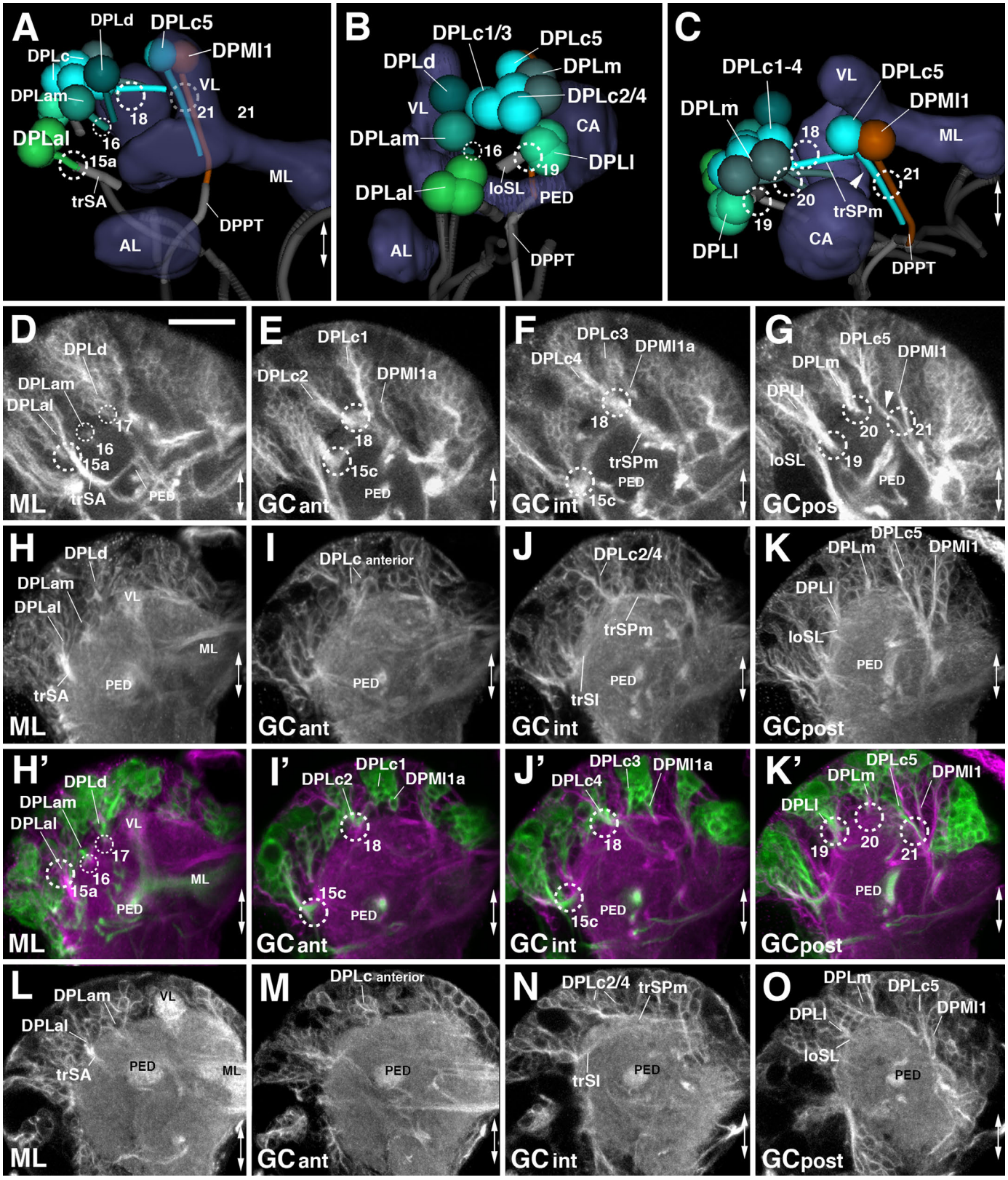


**Fig. 7.** Tracts associated with dorso-posterior lateral (DPL) lineages. (A–C) Digital 3D models of DPL lineages and tracts in a single L1 brain hemisphere. Anterior view (A), lateral view (B), dorsal view (C). Mushroom body and antennal lobe (blue-gray) and FasII-positive tracts (dark gray) are shown for reference. Numbered hatched circles in (A) and other panels represent entry portals of lineage-associated tracts. Double-headed arrow in (A, C) and all other panels indicates brain midline. (D–O) *z*-Projections of frontal confocal sections of a single brain hemisphere of early L3 (64 h; D–G), late L2 (48 h; H–K′), and L1 (12 h; L–O). Antero-posterior levels shown by *z*-projections are indicated by letters [ML, anterior GC level (GCant), intermediate GC level (GCint), posterior GC level (GCpost)] at lower left corner (for definition of levels, see Fig. 2). Secondary lineages are labeled by anti-Neurotactin (BP106; white in D–G) or *insc*-Gal4 > UAS-chRFP-Tub (green in H′–K′); primary neurons and tracts are labeled by anti-Neuroglian (BP104; white in H–K and L–O; magenta in H′–K′). For abbreviations of compartments and fiber tracts see Table 1; for numbering of entry portals see Table 2. Bar: 20 μm (D–O).

further posteriorly and ventrally one finds the DPLp group, which, because of their close association with the CP lineages, is discussed along with these (see below).

DPLc includes five lineages (DPLc1-5) at the secondary stage (second to third larval instar; Fig. 7D–G). The cell body clusters are spread out over a fairly wide area topping the superior lateral protocerebrum (SLP); tracts converge on a thick bundle (called the medial transverse superior posterior fascicle; trSPm) that forms a conspicuous entry portal at the boundary between the SLP and superior medial protocerebrum (SMP; Pereanu and Hartenstein, 2006; Lovick et al., 2013; Fig. 7F). Within the neuropil, DPLc tracts have a medially directed trajectory that passes towards and then underneath the longitudinal superior medial fascicle (loSM). DPLc2 and 4 reach the neuropil from a more lateral position, and form a more posterior tract than DPLc1/3/5 (Fig. 7D–G). The cell body clusters of DPLc2 and DPLc1 (Fig. 7E) are located anteriorly of DPLc3/4/5 (Fig. 7F, G). A characteristic feature of DPLc5 is its possession of a second, ventrally directed tract (Fig. 7C, G, arrowhead) which enters the posterior neuropil at the CA m portal (#21 in Figs. 2J and 7C, K′). This configuration of DPLc lineages can be followed backward from late L3 to approximately 48 h post-hatching, when secondary tracts start to elongate (Fig. 7H-K′). Prior to this stage, primary DPLc tracts form one thick bundle that passes superficially from laterally to medially over the SLP (trSPm in Figs. 2K4 and 7A, C, N). This bundle, fed by a more lateral and a more medial cluster, corresponds to the DPLc2/4 tract. Expression of FasIII in DPLc2/4 throughout the larval period (Supplementary Fig. S5) helps identifying these DPLc members in the early larval brain. Further anteriorly are clusters with very short axon bundles directed towards the DPLc2/4 tract; these clusters (DPLc anterior in Fig. 7I, M) are interpreted as DPLc1/3. For DPLc5, a substantial ventrally-directed tract, which projects parallel to the descending DPMl1 tract (Fig. 7A, C, G, K/K′, O; see also below) can be distinguished.

DPLm1/2 form a pair located posterior of the DPLc group, laterally adjacent to the calyx (Figs. 2K4, K5 and 7B, C, G, K, O). A short tract enters at SLP p (#20 in Figs. 2H, I and 7C, G, K′) and projects anteriorly at the boundary between the superior lateral and superior medial protocerebrums (SLP, SMP). One remaining DPL lineage, DPLd, is difficult to identify in the L1 brain. The secondary DPLd lineage enters laterally adjacent to the tip of the vertical lobe (entry portal VL dl, #17 in Fig. 7D, H′), and has a characteristic branched tract, with one branch projecting medially around the tip of the VL towards the midline, and the other branch directed postero-laterally towards the intermediate superior transverse fascicle (trSl). In the L1 brain, we can only identify a small cell cluster located laterally to the VL tip that corresponds in position to DPLd (Fig. 7A, H/H′).

### 3.8. Posterior-medial lineages: DPM and CM

The DPM and CM lineages are clustered along the dorso-medial-posterior edge of the superior medial protocerebrum (SMP). Among the DPMs, one can further distinguish, based on distinct projection pattern, a medial group (DPMm1/m2, DPMpm1/2) from two lateral groups (DPMl1/2, DPMpl1-3). The medial DPM lineages (except for DPMm2) are marked by the expression of several known driver lines (9D11-Gal4, Bayraktar et al., 2010; Riebli et al., 2013 and R13A10-Gal4 (see Table 2)) and represent Type II lineages which, at the secondary stage, produce much larger progeny by means of intermediate progenitors (Bello et al., 2008; Yang et al., 2013). DPMpm1 and DPMpm2 also express Fasciclin III throughout larval development (Supplementary Fig. S5B, C, E, F). These lineages, together with CM4 (see below), generate the columnar neurons of the central complex; following the nomenclature of Bello et al. (2008) they were called DM1-4, respectively). In the L1 brain, DPMm1, DPMpm1/2, and CM4 form already larger clusters than other (Type I) lineages. DPMm1/DM1 enters close to the dorsal midline at the PB m entry portal (#26 in Figs. 2J and 8A–C). Towards posterior-laterally it is followed by DPMpm1/DM2 and DPMpm2/DM3 which form the PB dl portal (#27 in Figs. 2J and 8A–D). These two lineages are also positive for the adhesion molecule Fasciclin III, which is expressed in a discrete subset of lineages throughout larval development (Fig. S2B, C, E, F).

Each one of the three medial DPM Type II lineages has a tract that follows an antero-ventral trajectory into the posterior inferior protocerebrum (IPp), before turning medially towards the midline (Figs. 2K4, K5 and 8A, B). The convergence of medially-directed fibers of DPMm1, DPMpm1/2, and CM4 (see below) represents the primordium of the fan-shaped body (prFB), as recently defined by Riebli et al. (2013) who used a Gal4 driver line specifically expressed in primary neurons of these four lineages. Aside from the tract destined for the primordium of the fan-shaped body, DPMpm1/2 produce a second axon bundle that has a projection identical to that described for the corresponding secondary lineages (Lovick et al., 2013): DPMpm2 axons project antero-laterally into the longitudinal superior medial fascicle (loSM); DPMpm1 axons follow the antennal lobe tract antero-ventrally (ALT; Fig. 8A). DPMm1 also forms a second tract, directed medially and crossing the midline at a level posterior to the primordium of the fan-shaped body (Fig. 8A, B). A similar tract is formed by the secondary DPMm1 lineage (Lovick et al., 2013), in addition to several other tracts that are not distinguishable in the early larva. The fourth member of the medial DPMs, DPMm2, is located lateral of DPMpm1 and enters at PB dl (#27); it is negative for the Type II lineage marker 9D11-Gal4 and projects medially (Fig. 8A–D).

Two lineages, DPMpl1 and DPMpl2, are situated postero-laterally adjacent to DPMpm2. Their entry portal, CA m (#21 in Figs. 2H, J and 8A, B, D), is located right next to the PB dl entry portal. Axons of DPMpl1/2 (which form a single cell cluster at the L1 stage) converge onto a forward directed tract that defines the longitudinal superior medial fascicle (loSM; Fig. 8A–E). DPMpm2 also sends a branch into this fascicle (arrow in Fig. 8D), similar to DPMpm2 at the secondary stage (Lovick et al., 2013). The third DPMpl lineage, DPMpl3, is located ventrally of DPMpl1/2 and projects its tract along the medial equatorial fascicle (MEF; entry portal PB v, #28; Figs. 2J, K5 and 8A, B, D, E, H).

The second lateral DPM group, DPMl, is represented by one lineage (DPMl1) with a thick, highly visible tract. DPMl1 is located at the level of DPMpl1/2 and DPMpm1/2, and extends its axons straight vertically, entering along with DPMpl1/2 via CA m (#21 in Figs. 2H, J and 8A, B, D). The DPMl1 axons define the FasII-positive dorso-posterior protecerebral tract (DPPT; a subset of DPMl1 neurons are positive for FasII; see Fig. 3C, F). The DPPT is accompanied by the equally massive axon bundle of DPLc5, which runs laterally parallel to it (Fig. 7C, G, K′). A thin fiber bundle converges on the DPMl1 tract from anteriorly. The cell body cluster, designated DPMl1a in Fig. 7E, F, I′, J′, giving rise to this bundle lies directly anterior to DPMl1. A definitive secondary lineage (represented by a clone) had not been defined previously; it is possible that DPMl1a represents a second primary lineage.

The CM lineages CM1, CM3, and CM4 are Type II lineages located at the postero-medial surface of the brain. Their short axon bundles converge upon two entry portals, a dorsal one (PB v; #28 in Figs. 2H, J, K5 and Fig. 8A, B, D, E) and a ventral one (VMC po; #29 in Figs. 2J, K5 and 8A, B, D, E). The dorsal convergence (CMd; Fig. 8A, B) is mostly formed by fibers of CM4, the fourth Type II lineage that, during the secondary stage, generates the columnar neurons of the central complex. CM4 axons form a thick bundle extending forward into the inferior protocerebrum; this bundle defines the medial equatorial fascicle (MEF; Figs. 2K4 and 8A–H). A branch of these forward-directed axons turns medially towards

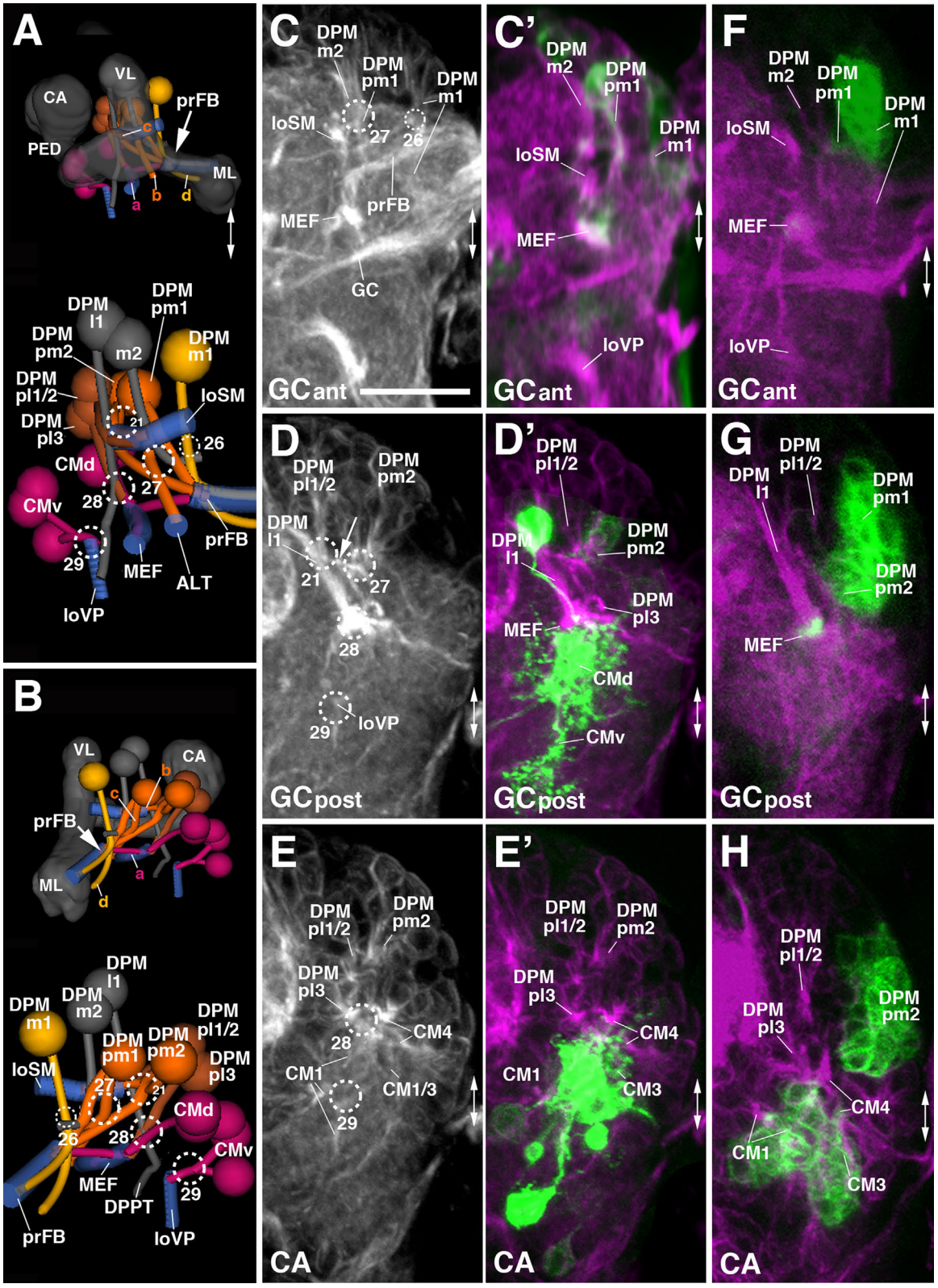


**Fig. 8.** Tracts associated with dorso-posterior medial (DPM) and centro-medial (CM) lineages. (A, B) Digital 3D models of DPM and CM lineages and tracts in a single L1 brain hemisphere. Anterior view (A), medial view (B). At top of each panel, lineages are shown in relationship to mushroom body (gray) for spatial orientation; bottom of panels shows higher magnification of lineages and neuropil tracts (light blue). Numbered hatched circles in (A) and other panels represent entry portals of lineage-associated tracts. Arrows in (A) and (B) point at convergence of tracts of DPMm1, DPMpm1/2, and CM4 to form a commissural tract that represents the primordium of the fan-shaped body (prFB). Letters "a"–"d" indicate additional tracts formed by these lineages (see text). Double-headed arrow in (A, C) and all other panels indicates brain midline. (C–H) *z*-Projections of frontal confocal sections of medial half of a L1 brain hemisphere (24 h; C–E′) and L2 larva (48 h; F–H). Antero-posterior levels shown by *z*-projections are indicated by letters (GCant, GCpost, CA) at lower left corner (for definition of levels, see Fig. 2). Primary neurons and tracts are labeled by anti-Neuroglian (BP104; white in panels C–E; magenta in C'-H). Primary neurons representing the Type II lineages DPMm1, DPMpm1/2, CM1/3/4 are labeled by 9D11-Gal4 > UAS-mcd8::GFP (green in C′–E′); from L2 onward, the same marker labels secondary neurons of these lineages (green in panels F–H). For abbreviations of compartments and fiber tracts see Table 1; for numbering of entry portals see Table 2. Bar: 20 μm (C–H).

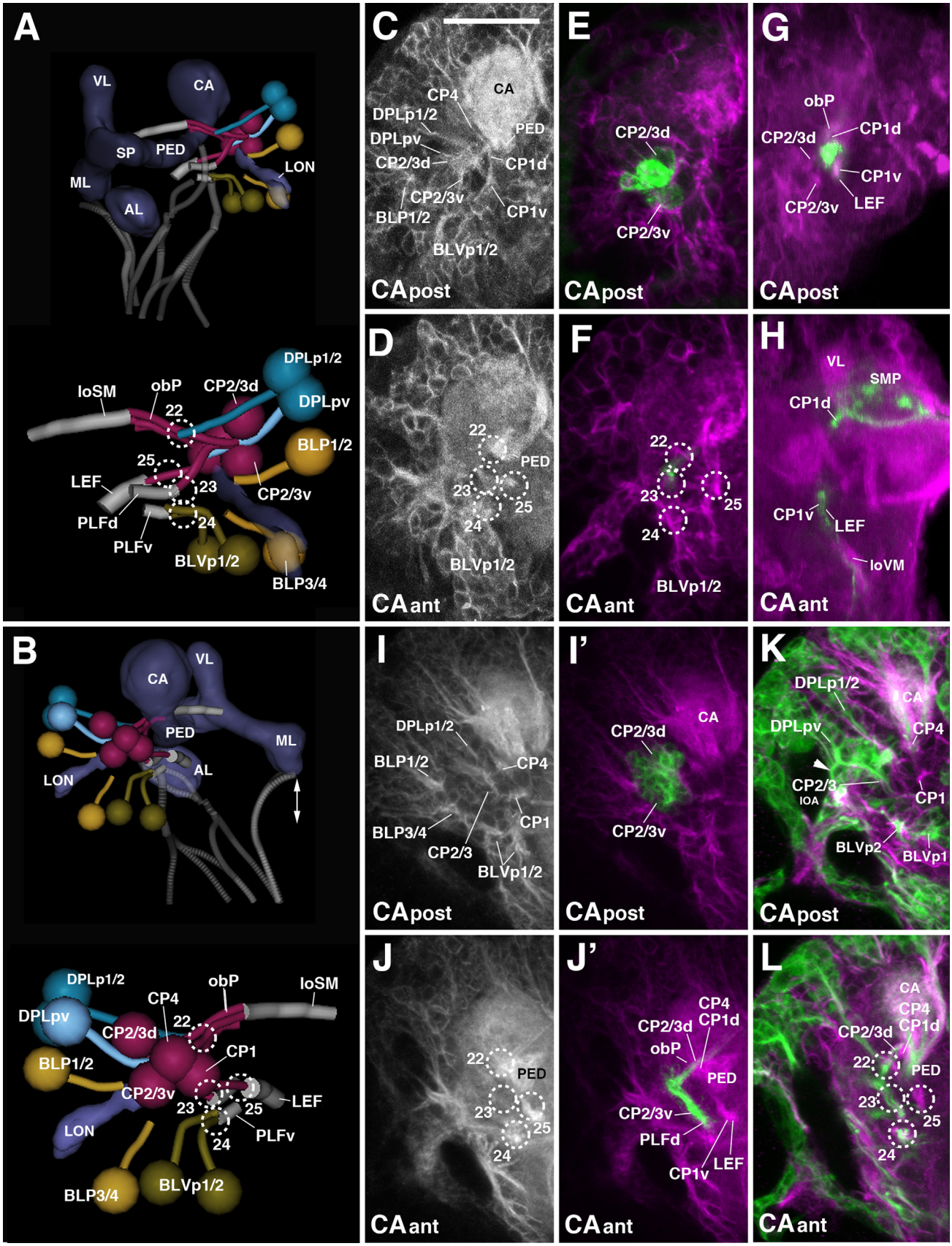


**Fig. 9.** Tracts associated with posterior lineages (CP, BLP, DPLp). (A, B) Digital 3D models of posterior lineages and tracts of a single L1 brain hemisphere. Lateral view (A), posterior view (B). At the top of each panel, lineages are shown in relationship to mushroom body (blue-gray) for spatial orientation; bottom of panels shows higher magnification of lineages and neuropil tracts (light blue). Numbered hatched circles in (A) and other panels represent entry portals of lineage-associated tracts. Double-headed arrow in (B) indicates brain midline. (C–L) *z*-Projections of frontal confocal sections of lateral half of brain hemisphere of L1 larva (24 h; C–H), L2 larva (48 h; I, J′), and early L3 larva (56 h; K, L). Lateral in all panels is to the left. Antero-posterior levels shown by *z*-projections are indicated by letters (CAant, CApost) at lower left corner (for definition of levels, see Fig. 2). Primary neurons and tracts are labeled by anti-Neuroglian (BP104; white in panels C, D, I, J; magenta in all other panels). Primary neurons representing the Type II lineages CP2 and CP3 are labeled by 9D11-Gal4 > UAS-mcd8::GFP (green in E, F); from L2 onward, the same marker labels secondary neurons of these lineages (green in panels I′, J′). Primary neurons of CP1 are labeled by R76A11-Gal4 > UAS-mcd8::GFP (green in G, H). Secondary neurons are globally labeled by *insc*-Gal4 > UAS-chRFP-Tub (green in K, L). For abbreviations of compartments and fiber tracts see Table 1; for numbering of entry portals see Table 2. Bar: 20 μm (C–L).

the primordium of the fan-shaped body (prFB; Fig. 8A, B). A second lineage projecting into the MEF is DPMpl3, located dorsally adjacent to CM4 (see above; Fig. 8A, B, E/E′, H). Extending anteriorly, the MEF splits up into branches that turn ventrally towards the great commissure (GC; Fig. 2K4), and antero-laterally towards the lateral accessory lobe (LAL; not shown).

Located ventrally and laterally of the origin of the medial equatorial fascicle (MEF) two clusters, interpreted as CM1 and CM3, have axons that contribute to the MEF, but mainly converge on the VMC po portal (#29) They project forward and ventrally, forming the longitudinal ventral posterior fascicle (loVP; Figs. 2J, K5 and 8A, B, D, E). The fifth CM lineage, CM5, a small Type I lineage located ventro-posteriorly extending its tract medially adjacent to CM4 at the secondary stage, could not be identified in L1 with certainty.

### 3.9. Posterior-lateral lineages: CP, DPLp, BLP, BLVp

The CP group comprises four lineages, CP1-4. Based on their expression of 9D11-Gal4, CP2 and CP3 represent Type II lineages (Bayraktar et al., 2010). CP2/3 form a thick tract that is located at the ventro-lateral boundary of the calyx and bifurcates into a dorsal and ventral branch (Figs. 2K5 and 9A–C, I, J′). The dorsal branch enters the neuropil at the CA l portal (#22 in Figs. 2I, J, K5 and 9A, B, D, F, J, L), and projects dorsomedially, forming the oblique posterior tract (obP; Fig. 9A, B, J′, L). The ventral branch projects anteriorly, parallel to the peduncle. This tract enters at the PLP ps portal (#23 in Figs. 2I, J, K5 and 9A, B, D, F, J, L) and forms the dorsal component of the posterior-lateral fascicle (PLFd; Fig. 9A, J′). CP1, marked by the expression of R76A11-Gal4 (Fig. 9G, H) enters medially of CP2/3 and also forms a branched tract (entry portal CA l, #22; Figs. 2I, J, K5 and 9B–D, F, G, J, L). The dorsal CP1 tract joins the obP, forming the ventral component of this thick bundle (Fig. 9A, B, J′, L). The ventral CP1 branch, which projects forward, medially of the ventral CP2/3 branch, enters at the CA v portal (#25 in Figs. 2J, K5 and 9A–D, J/J′, L) and forms part of the lateral equatorial fascicle (LEF; Figs. 2K4 and 9A, B, G, H, J′). The fourth CP lineage, CP4 (as defined at the secondary stage in the late larva), also projects along the obP, close to CP1; CP4 neurons and their primary tract are located dorsally of CP1 (entry portal CA l, #22; Figs. 2I, J, K5 and 9A–C, I, J/J′, K, L).

Three lineages of the DPL group, DPLp1/2 and DPLpv, are close to the CP clusters in location and projection. The DPLp1/2 cluster is located dorsally of CP2/3, laterally of the calyx (entry portal CA l; #22; Figs. 2I, J, K5 and 9A–D, F, I–L). The DPLp1/2 tract converges onto the dorsal CP2/3 tract as it turns into the oblique posterior tract (obP). DPLpv is located ventro-laterally of DPLp1/2, bordering the inner optic anlage of the optic lobe primordium (entry portal PLP ps, #23; Figs. 2I, J and 9D, F, J–L). At the secondary stage, DPLpv has a characteristic, bifurcated tract, with one short lateral branch towards the optic neuropil, and a medial branch that projects anteriorly along the posterior-lateral fascicle (PLFd), together with the CP2/3 axons (Fig. 9K, arrowhead). A primary cluster with a short, simple tract, projecting ventrally of the DPLp1/2 tract, can be followed back towards the L1 stage and has been tentatively defined as DPLpv (Fig. 9A–C).

BLP lineages are located at the postero-lateral brain surface, posteriorly of the optic lobe primordium. Their axon tracts approach the lateral neuropil surface (more precisely: the point where the lateral surface of the ventrolateral protocerebrum (VLP) is joined by the larval optic neuropil) from posteriorly (Pereanu and Hartenstein, 2006). At the secondary stage, BLPs form two lineage pairs with similar projection: BLP1/2, whose cell body clusters are located further dorsally, extend their axons antero-ventrally towards the lateral surface of the VLP compartment. BLP3/4, located further ventrally, project upward towards the lateral superior lateral protocerebrum (SLP; Lovick et al., 2013). Two BLP clusters with similar location and axonal trajectory can be followed backward towards the L1 stage: one cluster (termed BLP1/2) approaches the junction between the larval optic neuropil (LON) and VLP from postero-dorsally, the other one (BLP3/4) from postero-ventrally (Figs. 2I, J, K5 and 9A–D, F, I, J, L). Tracts cannot be followed any further anteriorly, and their entry portals into the brain neuropil cannot clearly be defined.

BLV lineages are located ventrolaterally of the optic lobe primordium. The two posterior-most members of this group, BLVp1/2, are located ventrally adjacent to CP2/3, and have closely apposed axon tracts that converge on the posterior-lateral fascicle carrying the ventral CP2/3 axons (PLF; Figs. 2K5 and 9A–D, I–L). BLVp1/2 tracts form a separate entry point (PLP pi; #24 in Figs. 2I, J, K5 and 9A–D, F, J, L) and continue as the ventral component of the PLF (PLFv) that projects anteriorly towards the lateral inferior protocerebrum.

### 3.10. Lateral lineages: BLA, BLD, BLV

BLA lineages are located along the anterior edge of the optic lobe primordium. At the secondary stage, they comprise a ventral group of 3 lineages (BLAv1/2, BLAvm) and a dorsal group of five lineages (BLAd1-4, BLAl). The BLAv lineages can be individually followed backward towards the L1 stage; primary BLAv lineages form three separate tracts that project posteriorly towards the lateral surface of the ventrolateral protocerebrum (VLP). Only BLAv1 is labeled by R67A11-Gal4 (Fig.10D/D′). The BLAv lineage tracts turn medially and enter the VLP neuropil (entry portal VLP dl, #32; Figs. 2I and 10A, B, D, E, G, H′, J, K); BLAv1/2 fibers continue medially as part of the great commissure (GC; Figs. 2K3 and 10A, B, D, E, G′, H′). BLAd lineages form a cluster dorsally of the BLAv lineages. Three to four short, posteriorly-directed tracts converge on a thick bundle which enters the superior lateral protocerebrum (SLP) at a position directly underneath the transverse superior anterior fascicle (trSA) formed by DPLal (entry portal SLP l, #15b; Figs. 2G–I, K3 and 10A–D, G/G′, J). Right posterior of the trSA, the BLAd bundle turns dorso-medially, forming the transverse superior intermediate fascicle (trSI; Fig. 10A–D). The BLAl lineage, located at the medial edge of the BLAd cluster, has a characteristic bifurcated tract that sends one branch postero-laterally, the other one antero-medially. The posterior branch follows the neuropil surface to join the axon bundle formed by BLAd; the antero-medial branch extends around the anterior neuropil surface along the boundary between the superior lateral protocerebrum (SLP) and ventrolateral protocerebrum (VLP), and approaches the spur of the mushroom body (Figs. 2K2, K3 and 10A, C).

BLD lineages are located dorsally of the optic lobe primordium and project tracts ventrally towards the lateral surface of the neuropil. At the secondary stage, six lineages, further subdivided into three pairs with similar trajectories, were identified. The posterior pair, BLD5/6, has long, vertically-oriented tracts that are directed towards the junction between the larval optic neuropil (LON) and the ventrolateral protocerebrum (VLP). Here, tracts turn medially in or near the great commissure (GC). The BLD5/6 pair, located furthest posteriorly and marked by R67A11-Gal4, can be followed backwards to the L1 stage (Figs. 2K4 and 10B, C, F/F′, I/I′, L). The PAT of this pair projects straight ventrally and enters the lateral neuropil immediately dorsal of the larval optic neuropil (LON; PLP l entry portal, #30; Figs. 2I and 10B, F, I/I′, L). The four anterior BLD lineages, BLD1-4, have tracts that approach the lateral surface and make a characteristic sharp turn towards dorso-medially, joining the transverse superior intermediate fascicle (trSI) formed by BLAd (see above). At the secondary stage, the BLD1-4 lineages have characteristic branching patterns, which do

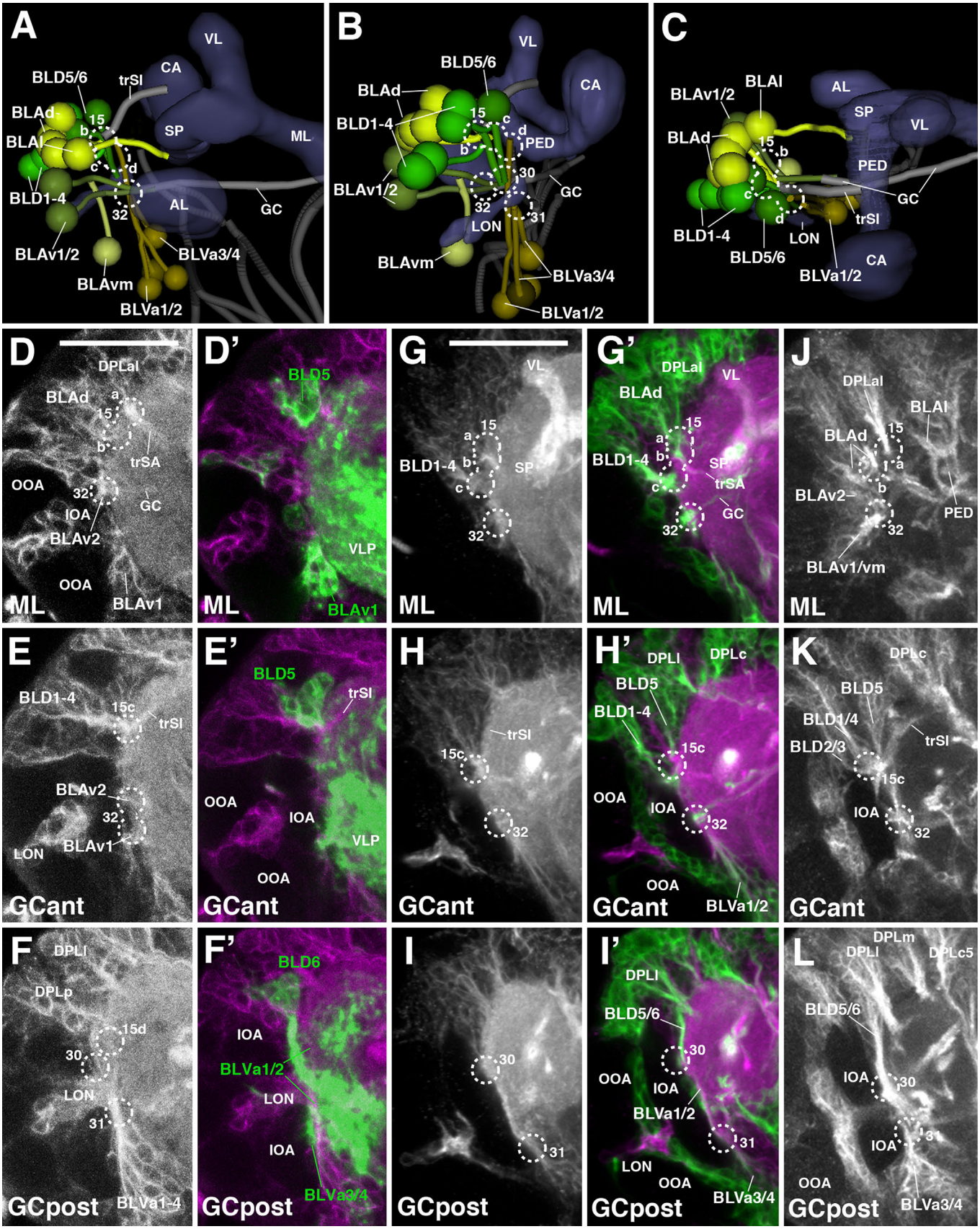


**Fig. 10.** Tracts associated with lateral lineages (BLA, BLD, BLV). (A–C) Digital 3D models of BL lineages and tracts in a single L1 brain hemisphere. Anterior view (A), postero-lateral view (B), dorsal view (C). Aside from mushroom body and antennal lobe (blue-gray) and FasII-positive tracts (dark gray), the larval optic neuropil (LON) is shown for reference. Fiber bundles of neuropil to which BL lineage tracts contribute are shown in light gray. Numbered hatched circles in (A) and other panels represent entry portals of lineage-associated tracts. (D–L) *z*-Projections of frontal confocal sections of lateral half of L1 brain hemisphere (24 h; D–F′) and early L3 larva (64 h; G–L). Lateral in all panels is to the left. Antero-posterior levels shown by *z*-projections are indicated by letters (ML, GCant, GCpost) at lower left corner (for definition of levels, see Fig. 2). Primary neurons and tracts are labeled by anti-Neuroglian (BP104; white in panels D–F and G–I; magenta in D′–F′ and D′–I′). Primary neurons of BLD5, BLD6, BLVa3, and BLVa4 are labeled by R67A11-Gal4 > UAS-mcd8::GFP (green in D′–F′). Secondary neurons are globally labeled by *insc*-Gal4 > UAS-chRFP-Tub (green in G′–I′) and anti-Neurotactin (BP106; white in J–L). On all panels, parts of larval optic lobe neuropil (LON) are shown close to left margin (IOA inner optic anlage; OOA outer optic anlage). For abbreviations of compartments and fiber tracts see Table 1; for numbering of entry portals see Table 2. Bar: 20 μm (D–F′); 50 μm (G–I′).

not exist at the primary stage in the L1 brain. Here, BLD1-4 form a lateral and a medial pair, directly adjacent to the dorsal edge of the optic lobe primordium (inner optic anlage, IOA; Fig. 10B, C, E, H/H′, K); axons of both clusters converge and enter the superior lateral protocerebrum (SLP) right next to the DPLal and BLAd tracts (SLP l entry portal, #15c; Figs. 2G, I and 10B, C, E, H/H′, K). BLD1-4 tracts continue along the trSI fascicle.

BLV lineages are grouped around the ventral edge of the optic lobe primordium and project their tracts dorsally, into the cleft formed in between the inner optic anlage (IOA) and the ventral lateral protocerebrum neuropil (VLP; Figs. 2K4 and 10A, B, F/F′, I/I′, L). The two posterior BLVs (BLVp1/2) were discussed in the previous section (see above). The remaining, anterior BLV lineages form two pairs, BLVa1/2 and BLVa3/4. The BLVa3/4 pair is located posteriorly and medially of the BLVa1/2 pair. As described for the corresponding secondary lineages, the primary BLVa3/4 tract is shorter, ending below the LON–VLP junction at the lateral surface of the VLP (entry portal VLP vl, #31; Figs. 2I, K4 and Fig. 10A, B, F/F′, I/I′, L). The BLVa1/2 tract extends further dorsally, passing anterior of the LON–VLP junction towards the superior lateral protocerebrum (SLP; entry portal LH a, #15d; Figs. 2G–I, K4 and 10A, B, F/F′, I/I′, L).

## 4. Discussion

### 4.1. The use of pan-neuronal markers in reconstructing brain architecture

The brain neuropil of insects and most other invertebrates is composed of the thin processes of neurons and glial cells. One can distinguish neuropil domains where terminal axonal and dendritic branches form synaptic connections (synaptic neuropil) from bundles of long processes (tracts or fascicles) that interconnect different domains of synaptic neuropil. Globally expressed neuronal membrane proteins, such as Neuroglian or Neurotactin, are concentrated in long axon bundles and, when labeled by protein-specific antibodies, they stand out against the surrounding synaptic neuropil. It is important to note that many known pan-neuronal proteins are expressed dynamically (Fung et al., 2008). Both Neurotactin and Neuroglian appear at high levels in young neurons that send out their initial axon during embryonic development (Bieber et al., 1989; Hortsch et al., 1990). As shown in the present study, the proteins are still highly expressed by all primary neurons in the early larva, but there are already differences in expression level which are most likely correlated with the birthdate of neurons. Thus, the intensity of labeling of neuronal cell bodies in the cortex is not identical for all cells; clusters of strongly labeled cell bodies, always closely associated with the beginning of the lineage axon tract (PAT), are surrounded by more weakly labeled cell bodies (see, for example, clusters indicated by arrows in Fig. 2L2). We suspect that the cells with higher expression levels are the late born neurons and that their strongly labeled axon tracts form the visible “backbone” of the PATs visible in the L1 brain. In the late larval brain, primary neuron expression of Neurotactin and (to a lesser extent), Neuroglian, wanes, while expression of these markers in secondary axon tracts is very robust. Secondary tracts maintain expression of Neurotactin and Neuroglian throughout early metamorphosis; at late pupal stages, Neuroglian remains strong all the way into adulthood, which makes it possible to relate the long axon tracts of the larva to those of the adult (Lovick et al., 2013).

One needs to point out that, aside from the lineage-associated axon bundles, there exists a second type of tract or fascicle which consists of less tightly packed parallel fibers with interspersed short terminal branches and synapses. A prominent example are the longitudinal, FasII-positive axon tracts of the ventral nerve cord and the lobes of the mushroom body. The long nerve fibers that scaffold these domains, also called “tract neuropils” (Virtual Fly Brain; Milyaev et al., 2012), are not necessarily related by lineage. This is very clear in case of the longitudinal tracts of the VNC, where lineage associated tracts form predominantly transverse (commissural) or vertical bundles (Kuert et al., 2014; Truman et al., 2004), but do not become part of the FasII-positive longitudinal fascicles. Instead, these fascicles are most likely formed by single or small subsets (“sublineages”) of axons belonging to several different lineages. In the embryo, FasII is expressed in groups of neurons that are born and differentiate early and thereby establish neuropil “pioneer” or “founder” tracts (Goodman and Doe, 1993; Nassif et al., 1998). The exact relationship of the FasII-positive neuron clusters to lineages has not yet been established; however, it seems clear that these clusters are derived from multiple lineages.

### 4.2. Factors controlling the spatial pattern of lineages and lineage-associated tracts

The pattern of PATs reflects in part the pattern of neuroblasts that had generated the lineages giving rise to the PATs. Based on clonal analysis, neuronal cell bodies belonging to one lineage cluster around their mother neuroblast and the PAT begins at the base of each cluster (Bossing et al., 1996; Larsen et al., 2009; Schmidt et al., 1997). There is no large scale migration of cell bodies away from the location in which they were placed at birth. The differences that one observes between the position of lineages in early and late embryos are brought about by a general movement of the brain primordium as a whole, whereby the neuraxis tilts posteriorly. For example, neuroblasts of lineages that are located dorso-posteriorly in the larval brain (e.g., mushroom body) start out quite anteriorly in the neuroblast map of the stage 11 embryo (Chang et al., 2003; Kunz et al., 2012; Noveen et al., 2000). It is not known what kind of morphogenetic mechanisms cause this shift; most likely, forces outside the brain primordium itself, such as the moving foregut and head epidermis, are involved. However, in terms of local neighborhood relationships between individual neuroblasts and the clusters of neurons they give rise to, there do not appear to be major changes between early and late embryonic stages (Chang et al., 2003; Sprecher et al., 2007).

Aside from neuroblast location, another determining factor of the pattern of PATs appears to be affinities of certain lineages to each other. Thus, PATs of most lineages do not enter the neuropil as individual bundles, but travel together in groups of 2–4 members. Such groups of entering PATs form “entry portals” that represent distinct landmarks at the neuropil surface. They appear as funnel-shaped depressions, or as clefts, in volume renderings of confocal stacks of preparations where the neuropil is labeled by global markers such as DN-cadherin (Figs. 2 and 11). Many portals form part of the boundaries between neuropil compartments; examples are the portals that surround the antennal lobe at the anterior neuropil surface. Importantly, the combinations of lineages that group together during the primary phase of neurogenesis remain in contact during secondary neurogenesis in the late larva. In other words, the entry portals defined by PATs in the L1 larva correspond to those formed by SATs in the adult brain (Lovick et al., 2013; Wong et al., 2013), which makes the entry portals a useful structural feature to follow neuropil morphogenesis throughout development (see below).

What do lineages that adhere together and enter the neuropil at the same portal have in common? Part of the answer probably lies in similarities in projection and connectivity mediated by the joined lineages. In the majority of cases, joined lineages project along the same fascicle within the neuropil, and therefore connect

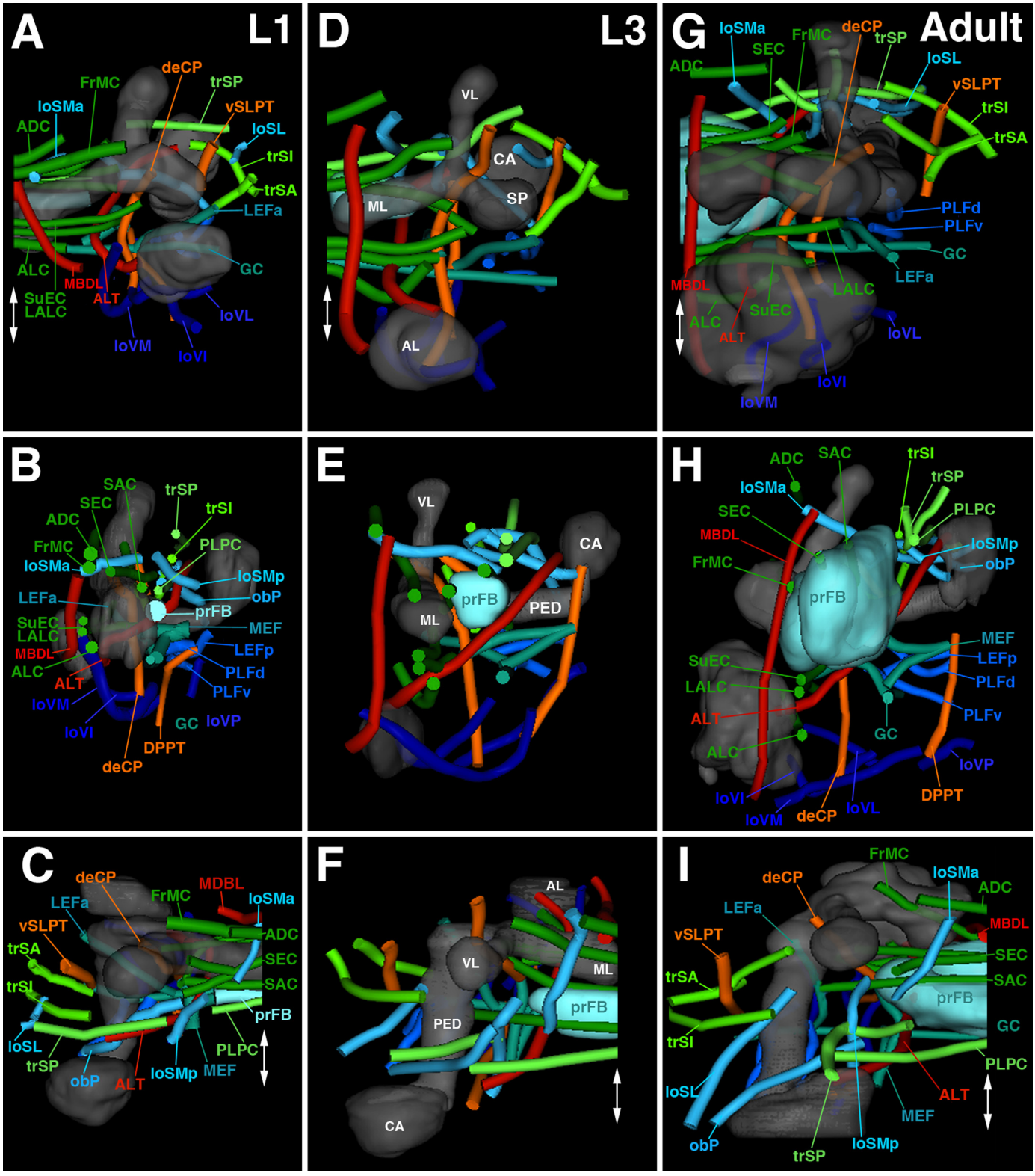


**Fig. 11.** Digital 3D models of lineage-associated neuropil tracts in a single hemisphere of the L1 larval brain, (A–C), L3 larval brain (D–F) and adult brain (G–I). Anterior view (upper row; A, D, G; medial to the left); medial view (intermediate row; B, E, H; anterior to the left); dorsal view (bottom row; C, F, I; medial to the right). Mushroom body and antennal lobe shown for reference (gray). Rendering of tracts follows color scheme used in Fig. 4 (longitudinal tracts: blue; transverse tracts/commissures: green; ascending tracts: red; descending tracts: orange). The fan-shaped body primordium is rendered in light blue. Double-headed arrow indicates midline. Bars: 20 μm (A–C); 25 μm (D–F); 50 μm (G–I).

overlapping or closely adjacent neuropil domains. Examples are BAmv1/2, BAlp2/3, BAla3/4, DALcl1/2 (hemilineages), DALcm1/2/DALd (hemilineages), DPLal1-3, DPLc1-5, DPLl1-3, BLAd1-4, BLP3/4, and BLV3/4. The secondary components of all of these lineages have been visualized as GFP-labeled clones, and show not only common tracts, but also similar, largely overlapping domains of terminal arborization (Ito et al., 2013; Wong et al., 2013; Yu et al., 2013). It will be interesting to establish for these groups of lineages

the corresponding neuroblasts and their genetic identities; one would expect that the commonalities in anatomical properties of a group are reflected in the expression of similar genes during early development.

### 4.3. Structural elements of the L1 and adult brain: a comparison

We had documented in previous studies (Nassif et al., 1998, 2003; Pereanu et al., 2010; Younossi-Hartenstein et al., 2006) that many structural elements of the adult brain can be already

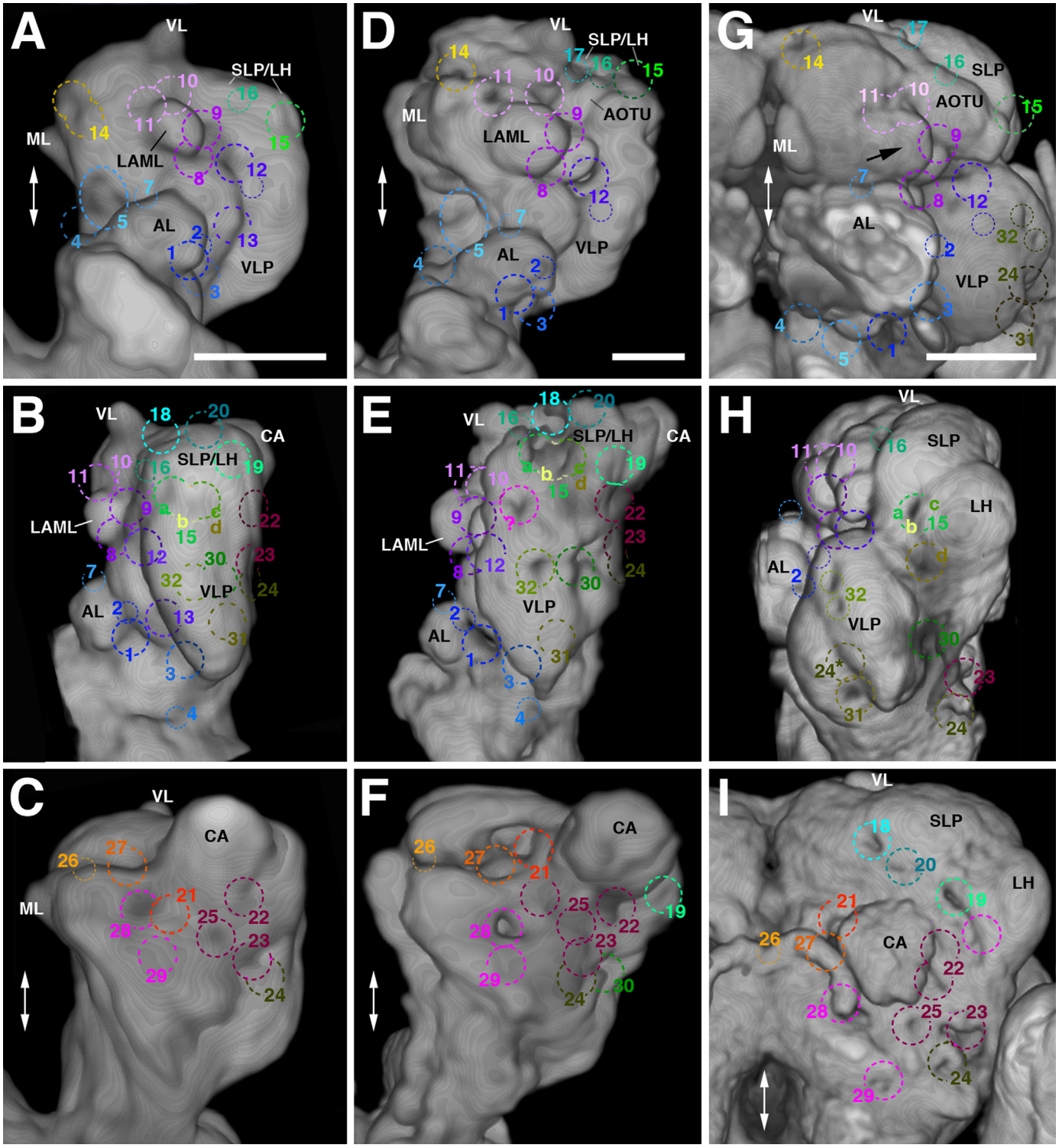


**Fig. 12.** Entry portals of lineage-associated tracts (numbered hatched circles in the L1 larval brain (A-C), L3 larval brain (D–F), and adult brain (G–I)). Each panel shows volume rendering of anti-DN-cadherin-labeled (L1) or anti-bruchpilot (L3, adult) brain hemisphere, highlighting relief of neuropil surface. Anterior view (upper row; A, D, G; medial to the left); lateral view (intermediate row; B, E, H; anterior to the left); posterior view (bottom row; C, F, I; medial to the left). Double-headed arrow in (A) and all other panels indicates brain midline. Rendering of entry portals follows color scheme used to differentiate between groups of lineages in Figs. 1 and 5–10.

recognized at the early larval stage. The identification of lineages and their associated tracts add many new details to these findings. Thus, the change in distances between fiber tracts (Fig. 11) and lineage entry portals (Fig. 12) that occur during development reflect the changes in neuropil growth that occurs during larval and pupal development. This growth is due to the enlargement of primary neuronal arbors (from early to late larva) and the addition of secondary neurons (from early larva to adult). Neuropil growth is highly anisotropic: some compartments grow much more than others. Compartments that grow most are related to the highly increased number of sensory afferents that characterizes the transition from larva to adult (12 photoreceptors in the larva, ~6000 photoreceptors in the adult; 21 antennal olfactory afferents in the larva; ~1300 in the adult (Laissue and Vosshall, 2008)), and to the control of complex motor acts the adult fly is capable of. Neuropil growth is most pronounced in four regions of the central brain: (1) the ventrolateral protocerebrum and anterior anterior optic tubercle which receives higher order input from the optic lobe (visual system); (2) the antennal lobe, a primary sensory center for olfaction; (3) the superior lateral protocerebrum and lateral horn, which presumably serve as multimodal association centers; (4) the central complex which controls locomotor behavior.

(1) The growth of the ventrolateral protocerebrum can be best appreciated in the anterior and lateral/medial views of the neuropil presented in Figs. 11A–F and 12A–F, respectively. Note the increase in distance between the vertically oriented tracts deCP and DPPT, and in length of the longitudinally oriented ventral fascicles (loVL, loVM, loVP; Fig. 11D–F). The portals of the laterally entering lineages BLVa3/4 (#31) and BLVp1/2 (#24), which are right next to each other in the L1 brain (Fig. 12D), are pushed apart (Fig. 12E, F); the same change occurs for the entries of BLAv1/2 (#32) and BLD5/6 (#30). The anterior anterior optic tubercle (AAOTU) bulges out of the anterior surface of the larval SLP compartment (Fig. 12C).
(2) The adult antennal lobe develops at the dorsal margin of its larval counterpart, as described in previous works (ref). The enormous growth of this compartment can be appreciated by the increasing vertical and horizontal distance between the entry portals of dorsal projection neuron lineage BAmv3 (#7) and the ventrolateral lineages BAla1/2 (#1; Fig. 12A–C). The portal of BAmv1/2 (#5), and the location of the ventral longitudinal medial fascicle (loVM) formed by these lineages, shifts to a ventral position (Figs. 11A–C and 12A–C). The BAmas1/2 portal (#6) is also pushed ventrally and the median bundle (MBDL) formed by the BAmas1/2 lineages lengthens (Fig. 11A–C).
(3) The neuropil domain located dorso-laterally of the peduncle is relatively underdeveloped in the larval brain, compared to the adult. Here, the neuropil forms prominent bulges, the superior lateral protocerebrum (SLP) and lateral horn (LH). By contrast, in the larva, the corresponding domain ("SLP/LH" in Fig. 12C, F, I) is represented by a thin layer of neuropil. The growth of these compartments is reflected in the increasing distances between the entry portals of anterior DPL lineages [DPLal (#15), DPLam (#16)] and posterior DPL lineages [DPLc (#18), DPLm (#19), DPLl (#20); see Fig. 12D, E, I]. The DPLc and DPLl portals, occupying a lateral position in the larva (Figs. 11G, H and 12 D, E), have been pushed towards the posterior brain surface by the outgrowing SLP and LH (Figs. 11I and 12I).
(4) The central complex develops during metamorphosis, primarily through the differentiation of the massive number of columnar/small field neurons generated by the type II lineages DPMm1/DM1, DPMpm1/DM2, DPMpm2/DM3, and CM4/DM4 (Riebli et al., 2013; Yang et al., 2013). In the early larval brain, primary neurons of these lineages form a commissural bundle that crosses the midline right behind the medial lobe of the mushroom body (Fig. 11D, G). This commissure, which grows into a sizeable primordium of the fan-shaped body by the third larval instar (Riebli et al., 2013; Fig. 11E, H), foreshadows the position of the central complex as a set of compartments formed during pupal development by elaborate branching of secondary commissural fibers that "squeeze" in between the commissures formed by previously established primary neurons (the SuEC/LALC antero-ventrally, SEC and SAC antero-dorsally, GC ventrally, and PLPC postero-dorsally; Fig. 11D–F). An anteriorly located lineage, DALv2, contributes the (large field) ring neurons of the ellipsoid body that represents the anterior part of the central complex (Fig. 11F).

## Acknowledgments

We thank Dr. J. Truman for generous help in the screen for Gal-4 lines with expression in larval brain lineages. This work was supported by NIH Grant R01 NS054814 to V.H.

## Appendix A. Supplementary material

Supplementary data associated with this article can be found in the online version at http://dx.doi.org/10.1016/j.bios.2014.05.063.

## References

Asburner M., Drosophila: A Laboratory Manual, 1989, Cold Spring Harbor Laboratory Press, Cold Spring Harbor, NY.
Bayraktar, O.A., Boone, J.Q., Drummond, M.L., Doe, C.Q., 2010. Drosophila type II neuroblast lineages keep Prospero levels low to generate large clones that contribute to the adult brain central complex. Neural Dev. 5, 26. http://dx.doi.org/10.1186/1749-8104-5-26.
Bello, B.C., Izergina, N., Caussinus, E., Reichert, H., 2008. Amplification of neural stem cell proliferation by intermediate progenitor cells in Drosophila brain development. Neural Dev. 3, 5. http://dx.doi.org/10.1186/1749-8104-3-5.
Betschinger, J., Mechtler, K., Knoblich, J.A., 2006. Asymmetric segregation of the tumor suppressor brat regulates self-renewal in Drosophila neural stem cells. Cell 124, 1241–1253.
Bieber, A.J., Snow, P.M., Hortsch, M., Patel, N.H., Jacobs, J.R., Traquina, Z.R., Schilling, J., Goodman, C.S., 1989. Drosophila neuroglian: a member of the immunoglobulin superfamily with extensive homology to the vertebrate neural adhesion molecule L1. Cell 59, 447–460.
Birkholz, O., Rickert, C., Nowak, J., Cobanl, C., Technau, G.M., 2015. Bridging the gap between postembryonic cell lineages and identified embryonic neuroblasts in the ventral nerve cord of *Drosophila melanogaster*. Biol. Open 4 (4), 420–434.
Boll, W., Noll, M., 2002. The Drosophila Pox neuro gene: control of male courtship behavior and fertility as revealed by a complete dissection of all enhancers. Development 129, 5667–5681.
Bossing, T., Udolph, G., Doe, C.Q., Technau G.M., 1996. The embryonic central nervous system lineages of *Drosophila melanogaster*. I. Neuroblast lineages derived from the ventral half of the neuroectoderm. Dev. Biol. 179, 41–64.
Brody, T., Odenwald, W.F., 2005. Regulation of temporal identities during Drosophila neuroblast lineage development. Curr. Opin. Cell Biol. 17, 672–675.
Caldwell, J.C., Miller, M.M., Wing, S., Soll, D.R., Eberl, D.F., 2003. Dynamic analysis of larval locomotion in Drosophila chordotonal organ mutants. Proc. Natl. Acad. Sci. U.S.A. 100, 16053–16058.
Cardona, A., Saalfeld, S., Arganda, I., Pereanu, W., Schindelin, J., Hartenstein, V., 2010a. Identifying neuronal lineages of Drosophila by sequence analysis of their axon tracts. J. Neurosci. 30, 7538–7553.
Cardona, A., Saalfeld, S., Preibisch, S., Schmid, B., Cheng, A., Pulokas, J., Tomancak, P., Hartenstein, V., 2010b. An integrated micro- and macroarchitectural analysis of the Drosophila brain by computer-assisted serial electron microscopy. PLoS Biol. 8, e1000502.
Cardona, A., Saalfeld, S., Schindelin, J., Arganda-Carreras, I., Preibisch, S., Longair, M., Tomancak, P., Hartenstein, V., Douglas, R.J., 2012. TrakEM2 software for neural circuit reconstruction. PLoS One. 7, e38011.
Chang, T., Younossi-Hartenstein, A., Hartenstein, V., 2003. Development of neural lineages derived from the sine oculis positive eye field of Drosophila. Arthropod. Struct. Dev. 32, 303–317.
Choi, J.C., Park, D., Griffith, L.C., 2004. Electrophysiological and morphological

characterization of identified motor neurons in the Drosophila third instar larva central nervous system. J. Neurophysiol. 91, 2353–2365.
Colomb, J., Grillenzoni, N., Ramaekers, A., Stocker, R.F., 2007. Architecture of the primary taste center of *Drosophila melanogaster* larvae. J. Comp. Neurol. 502, 834–847.
Das, A., Gupta, T., Davla, S., Prieto-Godino, L.L., Diegelmann, S., Reddy, O.V., Raghavan, K.V., Reichert, H., Lovick, J., Hartenstein, V., 2013. Neuroblast lineage-specific origin of the neurons of the Drosophila larval olfactory system. Dev. Biol. 373, 322–337.
de la Escalera, S., Bockamp, E.O., Moya, F., Piovant, M., Jiménez, F., 1990. Characterization and gene cloning of neurotactin, a Drosophila transmembrane protein related to cholinesterases. EMBO J. 9, 3593–3601.
Dumstrei, K., Wang, F., Nassif, C., Hartenstein, V., 2003. Early development of the Drosophila brain. V. Pattern of postembryonic neuronal lineages expressing Shg/DE-cadherin. J. Comp. Neurol. 455, 451–462.
Friggi-Grelin, F., Coulom, H., Meller, M., Gomez, D., Hirsh, J., Birman, S., 2003. Targeted gene expression in Drosophila dopaminergic cells using regulatory sequences from tyrosine hydroxylase. J. Neurobiol. 54, 618–627.
Fung, S., Wang, F., Chase, M., Godt, D., Hartenstein, V., 2008. Expression profile of the cadherin family in the developing Drosophila brain. J. Comp. Neurol. 506, 469–488.
Gerber, B., Stocker, R.F., 2007. The Drosophila larva as a model for studying chemosensation and chemosensory learning: a review. Chem. Senses 32, 65–89.
Ghysen, A., Dambly-Chaudière, C., Jan, L.Y., Jan, Y.N., 1993. Cell interactions and gene interactions in peripheral neurogenesis. Genes Dev. 7, 723–733.
Goodman, C.S., Doe, C.Q., 1993. Embryonic development of the Drosophila central nervous system. In: Bate, M., Martinez-Arias, A. (Eds.), In the Development of *Drosophila melanogaster*. Cold Spring Harbor: Cold Spring Harbor Press, pp. 941–1012.
Grenningloh, G., RehmE., J., Goodman, C.S., 1991. Genetic analysis of growth-cone guidance in Drosophila: fasciclin II functions as a neuronal recognition molecule. Cell 67, 45–57.
Hartenstein, V., 1988. Development of the Drosophila larval sensory organs: spatiotemporal pattern of sensory neurones, peripheral axonal pathways, and sensilla differentiation. Development 102, 869–886.
Hartenstein, V., Spindler, S., Pereanu, W., Fung, S., 2008. The development of the Drosophila larval brain. Adv. Exp. Med Biol. 628, 1–31.
Hayashi, S., Ito, K., Sado, Y., Taniguchi, M., Akimoto, A., Takeuchi, H., Aigaki, T., Matsuzaki, F., Nakagoshi, H., Tanimura, T., Ueda, R., Uemura, T., Yoshihara, M., Goto, S., 2002. GETDB, a database compiling expression patterns and molecular locations of a collection of Gal4 enhancer traps. Genesis 34, 58–61.
Hortsch, M., Patel, N.H., Bieber, A.J., Traquina, Z.R., Goodman, C.S., 1990. Drosophila neurotactin, a surface glycoprotein with homology to serine esterases, is dynamically expressed during embryogenesis. Development 110, 1327–1340.
Ito, K., Hotta, Y., 1992. Proliferation pattern of postembryonic neuroblasts in the brain of *Drosophila melanogaster*. Dev. Biol. 149, 134–148.
Ito, M., Masuda, N., Shinomiya, K., Endo, K., Ito, K., 2013. Systematic analysis of neural projections reveals clonal composition of the Drosophila brain. Curr. Biol. 23, 644–655.
Ito, K., Shinomiya, K., Ito, M., Armstrong, J.D., Boyan, G., Hartenstein, V., Harzsch, S., Heisenberg, M., Homberg, U., Jenett, A., Keshishian, H., Restifo, L.L., Rössler, W., Simpson, J.H., Strausfeld, N.J., Strauss, R., Vosshall, L.B., 2014. A systematic nomenclature for the insect brain. Neuron 81, 755–765.
Jenett, A., Rubin, G.M., Ngo, T.T., Shepherd, D., Murphy, C., Dionne, H., Pfeiffer, B.D., Cavallaro, A., Hall, D., Jeter, J., Iyer, N., Fetter, D., Hausenfluck, J.H., Peng, H., Trautman, E.T., Svirskas, R.R., Myers, E.W., Iwinski, Z.R., Aso, Y., DePasquale, G. M., Enos, A., Hulamm, P., Lam, S.C., Li, H.H., Laverty, T.R., Long, F., Qu, L., Murphy, S.D., Rokicki, K., Safford, T., Shaw, K., Simpson, J.H., Sowell, A., Tae, S., Yu, Y., Zugates, C.T., 2012. A GAL4-driver line resource for Drosophila neurobiology. Cell Rep. 2, 991–1001.
Johansen, J., Halpern, M.E., Keshishian, H., 1989. Axonal guidance and the development of muscle fiber-specific innervation in Drosophila embryos. J. Neurosci. 9, 4318–4332.
Kaneko, M., Hall, J.C., 2000. Neuroanatomy of cells expressing clock genes in Drosophila: transgenic manipulation of the period and timeless genes to mark the perikarya of circadian pacemaker neurons and their projections. J. Comp. Neurol 422, 66–94.
Kim, M.D., Wen, Y., Jan, Y.N., 2009. Patterning and organization of motor neuron dendrites in the Drosophila larva. Dev. Biol. 336, 213–221.
Kohsaka, H., Okusawa, S., Itakura, Y., Fushiki, A., Nose, A., 2012. Development of larval motor circuits in Drosophila. Dev. Growth Differ. 54, 408–419.
Kuert, P.A., Bello, B.C., Reichert, H., 2012. The labial gene is required to terminate proliferation of identified neuroblasts in postembryonic development of the Drosophila brain. Biol. Open. 1, 1006–1015.
Kuert, P.A., Hartenstein, V., Bello, B.C., Lovick, J.K., Reichert, H., 2014. Neuroblast lineage identification and lineage-specific Hox gene action during postembryonic development of the subesophageal ganglion in the Drosophila central brain. Dev. Biol. 390, 102–115.
Kumar, A., Fung, S., Lichtneckert, R., Reichert, H., Hartenstein, V., 2009. Arborization pattern of engrailed-positive neural lineages reveal neuromere boundaries in the Drosophila brain neuropil. J. Comp. Neurol. 517, 87–104.
Kwon, J.Y., Dahanukar, A., Weiss, L.A., Carlson, J.R., 2011. Molecular and cellular organization of the taste system in the Drosophila larva. J. Neurosci. 31, 15300–15309.
Kunz, T., Kraft, K.F., Technau, G.M., Urbach, R., 2012. Origin of Drosophila mushroom body neuroblasts and generation of divergent embryonic lineages. Development 139, 2510–2522.
Lai, S.L., Awasaki, T., Ito, K., Lee, T., 2008. Clonal analysis of Drosophila antennal lobe neurons: diverse neuronal architectures in the lateral neuroblast lineage. Development 135, 2883–2893.
Laissue, P.P., Vosshall, L.B., 2008. The olfactory sensory map in Drosophila. Adv. Exp. Med. Biol. 628, 102–114.
Landgraf, M., Jeffrey, V., Fujioka, M., Jaynes, J.B., Bate, M., 2003a. Embryonic origins of a motor system: motor dendrites form a myotopic map in Drosophila. PLoS Biol. 1, E41.
Landgraf, M., Sánchez-Soriano, N., Technau, G.M., Urban, J., Prokop, A., 2003b. Charting the Drosophila neuropile: a strategy for the standardised characterisation of genetically amenable neurites. Dev. Biol. 260, 207–225.
Larsen, C., Shy, D., Spindler, S., Fung, S., Younossi-Hartenstein, A., Hartenstein, V., 2009. Patterns of growth, axonal extension and axonal arborization of neuronal lineages in the developing Drosophila brain. Dev. Biol. 335, 289–304.
Lee, T., Lee, A., Luo, L., 1999. Development of the Drosophila mushroom bodies: sequential generation of three distinct types of neurons from a neuroblast. Development 126, 4065–4076.
Liu, L., Yermolaieva, O., Johnson, W.A., Abboud, F.M., Welsh, M.J., 2003. Identification and function of thermosensory neurons in Drosophila larvae. Nat. Neurosci. 6, 267–273.
Lichtneckert, R., Bello, B., Reichert, H., 2007. Cell lineage-specific expression and function of the empty spiracles gene in adult brain development of *Drosophila melanogaster*. Development 134, 1291–1300.
Lovick, J.K., Ngo, K.T., Omoto, J.J., Wong, D.C., Nguyen, J.D., Hartenstein, V., 2013. Postembryonic lineages of the Drosophila brain: I. Development of the lineage-associated fiber tracts. Dev. Biol. 384, 228–257.
Lovick J.K., Kong A., Omoto J.J., Ngo K.T., Younossi-Hartenstein A., Hartenstein V., 2015. Patterns of growth and tract formation during the early development of secondary lineages in the Drosophila larval brain, Devel Neurobio. http://dx.doi.org/10.1002/dneu.22325.
Masuda-Nakagawa, L.M., Tanaka, N.K., O'Kane, C.J., 2005. Stereotypic and random patterns of connectivity in the larval mushroom body calyx of Drosophila. Proc. Natl. Acad. Sci. U.S.A. 102, 19027–19032.
Masuda-Nakagawa, L.M., Gendre, N., O'Kane, C.J., Stocker, R.F., 2009. Localized olfactory representation in mushroom bodies of Drosophila larvae. Proc. Natl. Acad. Sci. U.S.A. 106, 10314–10319.
Milyaev, N., Osumi-Sutherland, D., Reeve, S., Burton, N., Baldock, R.A., Armstrong, J. D., 2012. The virtual fly brain browser and query interface. Bioinformatics 28, 411–415.
Minocha, S., 2010. A Role of Pox Neuro in the Developing Drosophila Brain: Determination of Large-Field Neurons Essential for Ellipsoid Body Formation and of Ventral Projection Neurons (Doctoral dissertation). Retrieved from Zurich Open Repository and Archive.
Nassif, C., Noveen, A., Hartenstein, V., 1998. Embryonic development of the Drosophila brain I. The pattern of pioneer tracts. J. Comp. Neurol. 402, 10–31.
Nassif, C., Noveen, A., Hartenstein, V., 2003. Early development of the Drosophila brain III. The pattern of neuropile founder tracts during the larval period. J. Comp. Neurol. 455, 417–434.
Noveen, A., Daniel, A., Hartenstein, V., 2000. The role of eyeless in the embryonic development of the Drosophila mushroom body. Development 127, 3475–3488.
Pearson, B.J., Doe, C.Q., 2004. Specification of temporal identity in the developing nervous system. Annu. Rev. Cell Dev. Biol. 20, 619–647.
Pereanu, W., Hartenstein, V., 2006. Neural lineages of the Drosophila brain: a 3D digital atlas of the pattern of lineage location and projection at the late larval stage. J. Neurosci. 26, 5534–5553.
Pereanu, W., Kumar, A., Jenett, A., Reichert, H., Hartenstein, V., 2010. Development-based compartmentalization of the Drosophila central brain. J. Comp. Neurol. 518, 2996–3023.
Power, M.E., 1948. The thoraco-abdominal nervous system of an adult insect *Drosophila melanogaster*. J. Comp. Neurol. 88, 347–409.
Python, F., Stocker, R.F., 2002. Adult-like complexity of the larval antennal lobe of *D. melanogaster* despite markedly low numbers of odorant receptor neurons. J. Comp. Neurol. 445, 374–387.
Rajashekhar, K.P., Singh, R.N., 1994. Neuroarchitecture of the tritocerebrum of *Drosophila melanogaster*. J. Comp. Neurol. 349, 633–645.
Ramaekers, A., Magnenat, E., Marin, E.C., Gendre, N., Jefferis, G.S., Luo, L., Stocker, R. F., 2005. Glomerular maps without cellular redundancy at successive levels of the Drosophila larval olfactory circuit. Curr. Biol. 15, 982–992.
Riebli, N., Viktorin, G., Reichert, H., 2013. Early-born neurons in type II neuroblast lineages establish a larval primordium and integrate into adult circuitry during central complex development in Drosophila. Neural Dev. 8, 6. http://dx.doi.org/10.1186/1749-8104-8-6.
Rusan, N.M., Peifer, M., 2007. A role for novel centrosome cycle in asymmetric cell division. J. Cell Biol. 177, 13–20.
Siebert, M., Banovic, D., Goellner, B., Aberle, H., 2009. Drosophila motor axons recognize and follow a Sidestep-labeled substrate pathway to reach their target fields. Genes Dev 23, 1052–1062.
Selcho, M., Pauls, D., Han, K.A., Stocker, R.F., Thum, A.S., 2009. The role of dopamine in Drosophila larval classical olfactory conditioning. PLoS One 4, e5897.
Schindelin, J., Arganda-Carreras, I., Frise, E., Kaynig, V., Longair, M., Pietzsch, T., Preibisch, S., Rueden, C., Saalfeld, S., Schmid, B., Tinevez, J.Y., White, D.J., Hartenstein, V., Eliceiri, K., Tomancak, P., Cardona, A., 2012. Fiji: an open-source platform for biological-image analysis. Nat. Methods 9, 676–682.
Schleyer, M., Saumweber, T., Nahrendorf, W., Fischer, B., von Alpen, D., Pauls, D.,

Thum, T., Gerber, B., 2011. A behavior-based circuit model of how outcome expectations organize learned behavior in larval Drosophila. Learn. Mem. 18, 639–653.
Schmidt, H., Rickert, C., Bossing, T., Vef, O., Urban, J., Technau, G.M., 1997. Dev Biol. 189, 186–204.
Schrader, S., Merritt, D.J., 2000. Central projections of Drosophila sensory neurons in the transition from embryo to larva. J. Comp. Neurol. 425, 34–44.
Sink, H., Whitington, P.M., 1991. Early ablation of target muscles modulates the arborisation pattern of an identified embryonic Drosophila motor axon. Development 113, 701–707.
Spindler, S.R., Hartenstein, V., 2010. The Drosophila neural lineages: a model system to study brain development and circuitry. Dev. Genes Evol. 220, 1–10.
Spindler, S.R., Hartenstein, V., 2011. Bazooka mediates secondary axon morphology in Drosophila brain lineages. Neural Dev. 6, 16. http://dx.doi.org/10.1186/1749-8104-6-16.
Sprecher, S., Reichert, H., Hartenstein, V., 2007. Gene expression patterns in primary neuronal clusters of the Drosophila embryonic brain. Gene Expr. Patterns 7, 584–595.
Sprecher, S.G., Cardona, A., Hartenstein, V., 2011. The Drosophila larval visual system: high-resolution analysis of a simple visual neuropil. Dev. Biol. 358, 33–43.
Stocker, R.F., Heimbeck, G., Gendre, N., de Belle, J.S., 1997. Neuroblast ablation in Drosophila P[Gal4] lines reveals origins of olfactory interneurons. J. Neurobiol. 32, 443–456.
Tabata, T., Schwartz, C., Gustavson, E., Ali, Z., Kornberg, T.B., 1995. Creating a Drosophila wing de novo, the role of engrailed, and the compartment border hypothesis. Development 121, 3359–3369.
Truman, J.W., Bate, M., 1988. Spatial and temporal patterns of neurogenesis in the central nervous system of *Drosophila melanogaster*. Dev. Biol. 125, 145–157.
Truman, J.W., Schuppe, H., Shepherd, D., Williams, D.W., 2004. Developmental architecture of adult-specific lineages in the ventral CNS of Drosophila. Development 131, 5167–5184.
Tyrer, N.M., Gregory, G.E., 1982. A guide to the neuroanatomy of locust suboesophageal and thoracic ganglia. Philos. Trans. R. Soc. Lond. B 297, 91–123.
Urbach, R., Technau, G.M., 2003. Molecular markers for identified neuroblasts in the developing brain of Drosophila. Development 130, 3621–3637.
Urbach, R., Technau, G.M., 2004. Neuroblast formation and patterning during early brain development in Drosophila. Bioessays 26, 739–751.
Vactor, D.V., Sink, H., Fambrough, D., Tsoo, R., Goodman, C.S., 1993. Genes that control neuromuscular specificity in Drosophila. Cell 73, 1137–1153.
Wong, D.C., Lovick, J.K., Ngo, K.T., Borisuthirattana, W., Omoto, J.J., Hartenstein, V., 2013. Postembryonic lineages of the Drosophila brain: II. Identification of lineage projection patterns based on MARCM clones. Dev. Biol. 384, 258–289.
Yang, J.S., Awasaki, T., Yu, H.H., He, Y., Ding, P., Kao, J.C., Lee, T., 2013. Diverse neuronal lineages make stereotyped contributions to the Drosophila locomotor control center, the central complex. J. Comp. Neurol. 521, 2645–2662 (Spc1).
Younossi-Hartenstein, A., Nassif, C., Hartenstein, V., 1996. Early neurogenesis of the Drosophila brain. J. Comp. Neurol. 370, 313–329.
Younossi-Hartenstein, A., Salvaterra, P., Hartenstein, V., 2003. Early development of the Drosophila brain IV. Larval neuropile compartments defined by glial septa. J. Comp. Neurol. 455, 435–450.
Younossi-Hartenstein, A., Shy, D., Hartenstein, V., 2006. The embryonic formation of the Drosophila brain neuropile. J. Comp. Neurol. 497, 981–998.
Yu, H.H., Awasaki, T., Schroeder, M.D., Long, F., Yang, J.S., He, Y., Ding, P., Kao, J.C., Wu, G.Y., Peng, H., Myers, G., Lee, T., 2013. Clonal development and organization of the adult Drosophila central brain. Curr. Biol. 23, 633–643.